

ACKNOWLEDGEMENTS

The author wishes to express his appreciation to his advisor, Jay Johnson, for his guidance and support during the completion of this study.

Others acknowledged for their help include: A. J. Mason, Radar Lee and Steve Gross for their laboratory help, Sharon Crews for her help in statistical programming, and Harold Vandervort for his efforts in making and maintaining many pieces of equipment necessary for the study.

Special appreciation goes to the author's wife, Marcia M. Harris, for her continued support and sacrifice over the past five years of graduate study.

A final thanks goes to the funding agency, the National Science Foundation, who made the project possible.

TABLE OF CONTENTS

	<u>Page</u>
ACKNOWLEDGEMENTS	ii
TABLE OF CONTENTS	iii
LIST OF TABLES	v
LIST OF FIGURES	vi
LIST OF APPENDICES	viii
INTRODUCTION	1
REVIEW OF ANGULAR DISTRIBUTION FUNCTIONS	5
MATERIALS, METHODS, AND MODELS	14
Particleboards Used in the Study	14
Method for Estimating the Concentration Parameter	16
Simulation of Elastic Properties	18
Experimental Measurements	25
RESULTS AND DISCUSSION	28
Characterizing Orientation	28
Results of Model Simulations	32
Tension	32
Shear	38
Experimental Results	46
Boards with known distribution functions	46
Boards with unknown distribution functions	48
Poisson's ratio	48
MOE and MOR	50
Effects of particle length	50
Potlatch boards	50

	<u>Page</u>
Comparisons Between Theory and Experiment	53
Tension	53
Shear	60
SUMMARY AND CONCLUSIONS	64
REFERENCES	66
APPENDICES	67
VITA	74
ABSTRACT	

LIST OF TABLES

<u>Table</u>		<u>Page</u>
1	Elastic constants used in simulation models (Wood Handbook, 1974, Bodig and Goodman, 1975)	22

LIST OF FIGURES

<u>Figure</u>		<u>Page</u>
1	Illustration of the relationship between the concentration parameter, κ , and the degree of alignment of line segments	7
2	Calibration of concentration parameter of von Mises distribution to shape factor of truncated gaussian distribution	10
3	Relationship between length of mean vector and concentration parameter of von Mises distribution . . .	12
4	Illustration of sampling method showing fifty random sampling points superimposed on a portion of particleboard	17
5	Schematic representation of the strip model	19
6	Spring representation of a) unlayered model, and b) layered model	20
7	Schematic representation of shear model	24
8	Circular histograms showing the degree of orientation of the experimental boards (the measured angles were doubled	30
9	Tensile elastic modulus of white pine and aspen as a function of the degree of orientation	34
10	Standard deviations of white pine and aspen tensile elastic modulus as a function of the degree of orientation	35
11	Difference between the effective elastic modulus of the layered and unlayered models, $E_L^* - E_{UL}^* = \Delta E$. .	37
12	Plate shear model, with a) the element size equal to the particle size, and b) the particles divided into nine elements	39
13	Shear stresses present along the panel diagonal for various element sizes	41
14	Potential energy as a function of the number of elements in the shear model	42

<u>Figure</u>		<u>Page</u>
15	Shear stress distribution in elements of shear model for two betas	43
16	Shear modulus of white pine and aspen as a function of the degree of orientation	45
17	Experimental tensile elastic modulus for white pine and aspen as a function of the degree of orientation .	47
18	Poisson's ratio of WSU boards as a function of degree of orientation	49
19	MOE for WSU boards as a function of the degree of orientation	51
20	MOR for WSU boards as a function of the degree of orientation	52
21	Tensile elastic modulus of white pine as a function of the degree of orientation	54
22	Tensile elastic modulus of aspen as a function of degree of orientation	55
23	Specific tensile elastic modulus of white pine as a function of degree of orientation	57
24	Specific tensile elastic modulus of aspen as a function of degree of orientation	58
25	Specific tensile modulus of WSU boards as a function of the degree of orientation	59
26	Specific shear modulus for white pine as a function of the degree of orientation	61
27	Specific shear modulus for aspen as a function of degree of orientation	62
28	Specific shear modulus for WSU boards as a function of degree of orientation	63

LIST OF APPENDICES

<u>Appendix</u>		<u>Page</u>
A	Raw Data	67
B	Statistics Results	73

INTRODUCTION

Particleboard is manufactured by pressing small particles of wood, coated with an adhesive, into a dense mat. The arrangement, shape, and orientation of the anisotropic particles determine, to a great extent, the mechanical behavior of the board. Since the principal material direction changes from point to point inside the board in a non-regular manner, this type of composite material can be classified as a statistically heterogeneous material. A theoretical treatment of the physical behavior of this type of material has been given by Beran (1968). It is apparent from his work that probability density functions will be indispensable with regard to modeling the performance of these materials.

The mechanical behavior of particleboard is affected by many variables, including: resin content, pressing time, species used, and the size, shape, and arrangement of the particles. Since wood particles are anisotropic, it is apparent that the orientation of the principal material directions of the particles will greatly influence the mechanical and physical properties of the board. Indeed, research dealing with the effects of orientation have shown it to be of prime importance. Klanditz (1960) doubled the stiffness of particleboard by orienting the grain of the flakes in the direction of the load, and Brumbaugh (1960) tripled the stiffness of specially fabricated flakeboards when particle orientation was coincidental with load direction. Steinmetz and Polley (1974) reported that with highly oriented fiberboards, the elastic modulus was in the range of many clear lumber specimens. They also reported that by orienting only the surface mat, the elastic

modulus and the modulus of rupture were significantly increased. These and other studies indicate that particle orientation in particleboard is a variable whose manipulation can produce drastic changes in its mechanical behavior.

In order to learn more about the effects of particle orientation on the mechanical properties of particleboard, this study was undertaken with the following objectives.

1. To characterize the state of orientation of particles in particleboard.
2. To develop a method of determining the orientation of particleboard "in situ".
3. To evaluate the theoretical effects of orientation on the stiffness of particleboard through the use of mathematical models.
4. To determine the consistency of the models by comparing them with experimental data.

In reviewing previously published literature dealing with particle orientation, it was noted that information regarding the specification of orientation is particularly lacking. The attempts to characterize orientation have primarily been restricted to mechanical behavior characterizations. For example, by testing boards in bending within the proportional limit, a relative stiffness in the aligned (E_x) and cross (E_y) direction can be determined (Talbot, 1976). As the orientation increases, the ratio, E_x/E_y , increases. Although this method is an effective tool for characterizing relative orientations,

it has one major drawback. It does not lend itself to modeling. A major objective of this study was to seek an alternative method of characterizing particle orientation which would be effective in specifically defining the particle orientation "in situ", as well as being an effective tool for modeling.

In order to specifically define orientation, it must be recognized that each individual particle has a grain direction corresponding to the longitudinal axis of the tree from which the particle came. If each particle is assigned an angle equal to the deviation of its grain angle from a set reference direction, the orientation of the particleboard can be described as the distribution of particle angles. The approach taken in this study was to use directional distribution functions to specify the distribution of particle angles.

After developing a method to characterize particle orientation, experimental particleboards were constructed with known angular distributions. A method of measuring particle orientation "in situ" was developed and the angular distribution of the experimental boards estimated. A comparison of the known vs. estimated orientations was used to evaluate the sampling technique.

In order to determine the effects particle orientation could theoretically have on the stiffness of particleboard, computer models were developed. Models to estimate both tension and shear modulus were developed and the theoretical effects of particle orientation determined. The results were compared to actual experimental results.

Although somewhat simplistic by design, this study was undertaken to help establish the role of orientation in particulate systems made

up of anisotropic particles. It was felt that if success was achieved, the information gained in this study could be not only used to characterize particle orientation in particleboard, but to characterize the orientation of elements in any composite material.

REVIEW OF ANGULAR DISTRIBUTION FUNCTIONS

There are many types of distribution functions. They can be classified into two groups, (1) distribution functions designed for data with finite ranges, and (2) those designed for data with an infinite range.

Angular data is an example of data with a finite range. For example, if birds are released from a given point, and the bearing of their disappearance on the horizon recorded, the measurement would have a finite range from 0 to 2π (0 to 360 degrees). Mardia (1972) discusses a number of probability density functions (pdf's) for characterizing such data. One of these is the von Mises density function, as given by

$$g(\theta; \mu_0, \kappa) = \frac{1}{2\pi I_0(\kappa)} e^{\kappa \cos(\theta - \mu_0)} \quad (1)$$

where $0 < \theta < 2\pi$ and I_0 is the modified Bessel function of order zero.

The mean of the population of angles, θ , is given by μ_0 , and the degree of dispersion about μ_0 is specified by the concentration parameter, κ . For example, if the concentration parameter is equal to zero ($\kappa = 0$) the distribution is uniform over the range 0 to 2π (i.e. each angle has an equal chance of being selected). Where the parameter is very large ($\kappa = \infty$) all observations are equal to μ_0 .

The cumulative distribution function (cdf) of the von Mises pdf centered about μ_0 is

$$G(\theta; \mu_0, \kappa) = \frac{1}{2} + \frac{1}{2\pi} \left\{ \theta + 2 \sum_{n=0}^{\infty} \frac{I_n(\kappa)}{I_0(\kappa)} \frac{\sin(n\theta)}{n} \right\} \quad (2)$$

In the previous example about bird flights, each observation was recorded based on the direction of flight. Not all cases of angular data have directional measurements, hence, all angular data does not have the range 0 to 2π . For example, when measuring the angular deviation of long thin particles in particleboard from a given reference line, the particles have no directional properties (one end cannot be distinguished from the other). No distinction can be made between particles which differ by π radians (i.e., the particles whose angles are recorded as 0 and π are actually oriented the same). Thus, in this case, the range is 0 to π . This is termed "axial data". By simply doubling the axial data, a range of 0 to 2π can be achieved.

The axial form of the von Mises pdf is

$$g_2(\theta; \mu_0, \kappa) = \frac{1}{\pi I_0(\kappa)} e^{\kappa \cos 2(\theta - \mu_0)} \quad (3)$$

and the axial df, centered about μ_0 , is

$$G_2(\theta; \mu_0, \kappa) = \frac{1}{2} + \frac{1}{\pi} \left\{ \theta + \sum_{n=0}^{\infty} \frac{I_n(\kappa)}{I_0(\kappa)} \frac{\sin(2n\theta)}{n} \right\} \quad (4)$$

Again, the dispersion about the mean, μ_0 , is given by the concentration parameter, κ . Figure 1 illustrates the effect of the concentration parameter on the orientation of a set of lines. The distribution of angles of the lines in Figure 1 corresponds to the axial

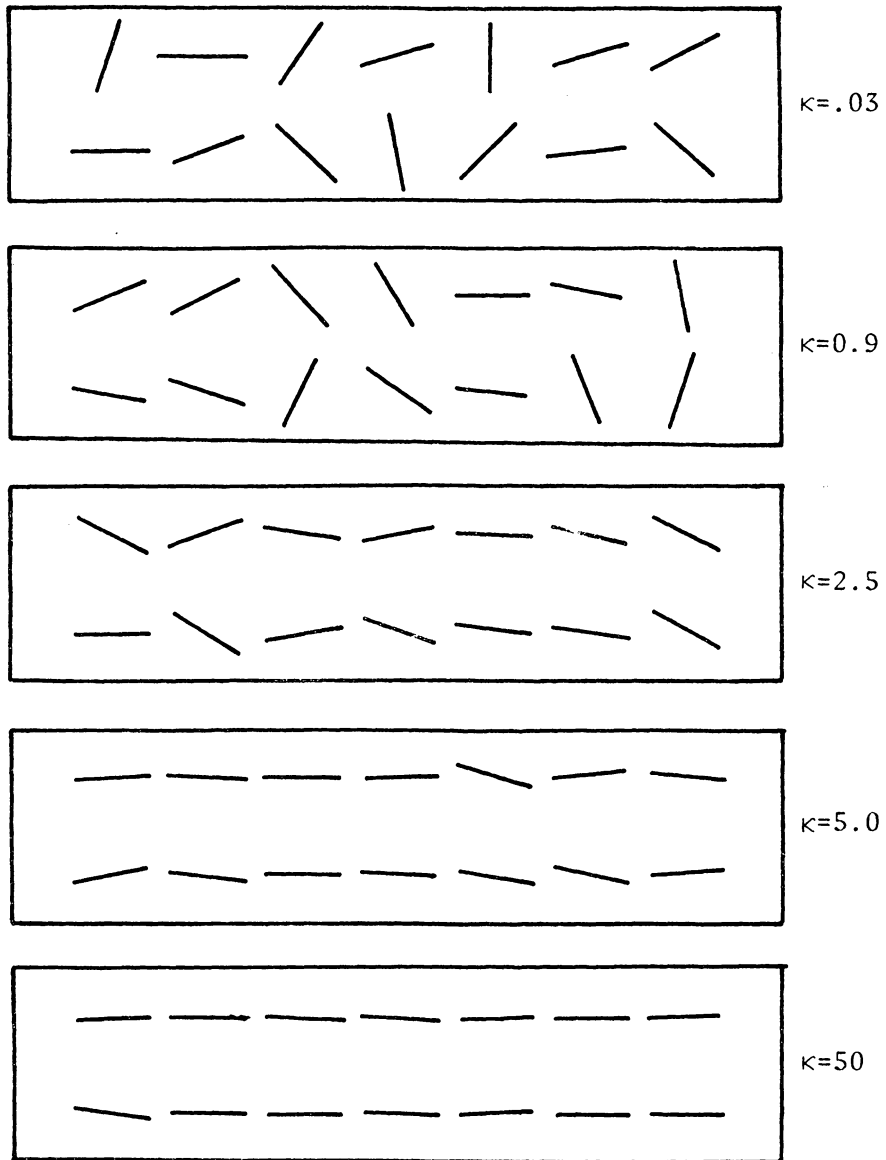


Figure 1. Illustration of the relationship between the concentration parameter, κ , and the degree of alignment of line segments.

von Mises df, with a range of $-\pi/2$ to $\pi/2$. The lines were plotted with reference to a horizontal line whose angle was assigned the value or 0. This illustration shows that the orientation can be specified by one parameter.

An exponential function, similar in form to the normal or gaussian distribution function used to characterize the central tendency of angular data is

$$f(\theta; \mu_0, \beta) = e^{-\beta^2(\theta - \mu_0)^2} \quad (5)$$

This function assumes an infinite range, and must be truncated to be used for finite ranges. It can be multiplied by a normalization factor,

$$NF = (\pi^{1/2}/\beta)\text{erf}(\beta\pi/2) \quad (6)$$

to obtain a truncated gaussian-type distribution function for axial data:

$$f(\theta; \mu_0, \beta) = \frac{\beta e^{-\beta^2(\theta - \mu_0)^2}}{\sqrt{\pi}\text{erf}(\beta\pi/2)} \quad (7)$$

such that all angles will be in the range 0 to π (0 to 180 degrees).

The mean of the population of angles, θ , is given by μ_0 , and the degree of dispersion about μ_0 is specified by the shape factor, β . The shape factor, β , corresponds to the concentration parameter, κ , or the von Mises distribution function.

The cumulative distribution function, center about $\mu_0 = 0$, is

$$F(\theta; 0, \beta) = \frac{1}{2} \left\{ 1 + \frac{\text{erf}(\beta\theta)}{\text{erf}(\beta\pi/2)} \right\} \quad (8)$$

As in the case of the von Mises distribution function, the truncated gaussian distribution function can be used to specify orientation by using only one number, the shape factor, β .

The von Mises and truncated gaussian distributions are actually quite similar (Johnson and Harris, 1976). The major discrepancy, although a small one, occurs at the ends of the interval. At that point, the von Mises pdf has a slope of zero, while the truncated gaussian pdf does not. For appropriate values of the concentration parameter and shape factor, therefore, the two pdf's are essentially the same.

The relationship between the concentration parameter and the shape factor is shown in Figure 2. The relationship between the two parameters for $\kappa > 2$ is given by

$$\beta = (2(\kappa - .5))^{1/2} \quad (9)$$

The portion of the curve where $\kappa < 2$, was obtained by adjusting the value of β , for a fixed value of κ , to minimize the sum of squares between the two df's.

Given these distribution functions to specify orientation, the next question is how to estimate the concentration parameter and shape factor "in situ". One simple, but effective method is discussed both in Mardia, 1972, and Batschelet, 1965. This method consists of estimating the mean vector, r_0 , or the angular measurements, θ , which

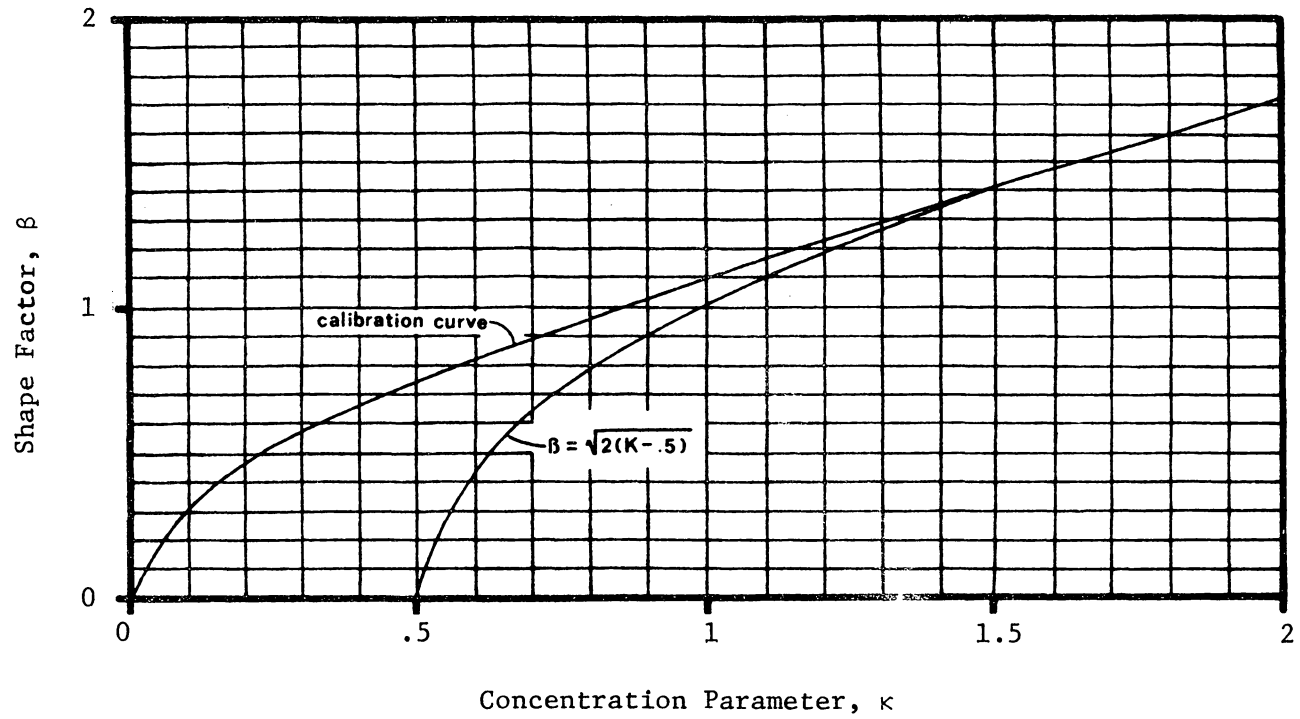


Figure 2. Calibration of concentration parameter of von Mises distribution to shape factor of truncated gaussian distribution.

is given by

$$r_o = (\overline{\cos^2\theta} + \overline{\sin^2\theta})^{1/2} \quad (10)$$

where: $\overline{\cos \theta}$ is the average cosine of the angles,

$\overline{\sin \theta}$ is the average sine of the angles.

If the angles are evenly distributed on the interval 0 to 2π , then the average sine and cosine will be zero, hence, the mean vector will be zero. If all angles are equal to the mean, the average sine and cosine will be equal to the sine and cosine of the mean angle, hence the mean vector will be equal to one. Thus, the mean vector, r_o , has a range of 0 to 1, and the dispersion around the mean angle is indicated by the magnitude of the mean vector. As the mean vector increases to 1, the dispersion around the mean angle decreases to 0.

The mean vector has been related to the concentration parameter, and thus, if the mean vector is known the concentration parameter can be found (Batschelet, 1965). The relationship between the concentration parameter and the mean vector is plotted in Figure 3. Actual values can be found in Table B of Batschelet, 1965. Since the relationship between the concentration parameter and the shape factor is known, it is apparent that the degree of orientation of a set of data can be found by simply estimating the mean vector, r_o .

In summary, two distribution functions appear to be effective in specifying orientation of a collection of angular measurements, the von Mises and the truncated gaussian distribution functions. These functions are useful in specifying orientation for two reasons: (1) the exact degree of orientation can be specified by a single parameter, and (2) that parameter can be estimated by making measurements "in

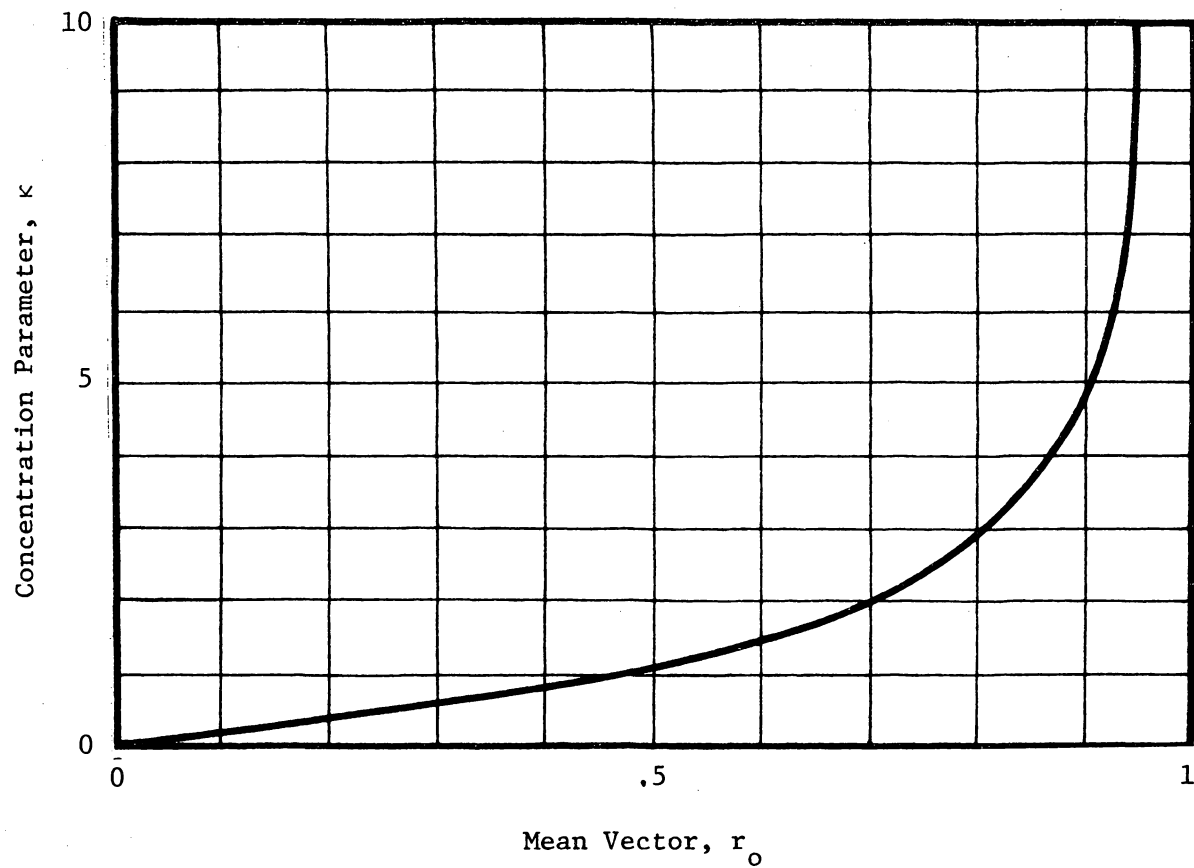


Figure 3. Relationship between length of mean vector and concentration parameter of von Mises distribution.

situ", calculating a mean vector r_0 and determining the concentration value from the relationship shown in Figure 3.

MATERIALS, METHODS AND MODELS

Particleboards Used in the Study

Three groups of boards were used in the study; boards with known distributions of particle angles, boards with unknown distributions of particle angles and a commercially produced particleboard with oriented particles.

Experimental boards with known distributions were constructed according to the following procedure. White pine (Pinus strobus L.) and quaking aspen (Populus tremuloides Mich.) were selected for use in making the experimental boards because of their fine texture, gradual transition from earlywood to latewood, as well as its good slicing characteristics. Flakes for the boards were cut from green blocks using a sliding microtome. The dimensions were 38 mm x 13 mm x .38 mm (1.5" x 0.5" x 0.015"). Care was taken to insure that the grain direction was coincident with the long axis of the particles. The flakes were pressed during drying to prevent curling. After drying, the particles were weighed and placed in a container with a pulverized 2-step phenolic glue manufactured by Varcum Chemicals (V6661-I-EX). The container was agitated thoroughly, and upon removal from the container, the particles were coated uniformly with the powdered glue, approximately 6 percent on a weight basis.

Experimental flakeboards were manufactured by individually laying down the coated particles in the form of a mat and then pressing at approximately 2.1 MPa (300 psi), with heat, 163°C (325°F), for 5 minutes to a thickness of 2 mm (.08"). The location of the particles

in the mat was determined by two random coordinates, each being generated from a uniform distribution function. The angular orientation of the long axis of the particle relative to the principal board direction was specified by a random angle generated from the truncated gaussian distribution, Equation 8. The angle was obtained by first selecting a random number, uniform on the unit interval, and then using this value to solve for a corresponding angle given by the inverse of the cumulative truncated normal distribution. Newton's method of successive approximations was used to determine the angles from the random numbers. A listing of the computer program for this procedure is given in Johnson and Harris, 1976. Six experimental boards were constructed with varying degrees of orientation: the shape factor, $\beta = 0.1, 1.0, 2.0, 3.0, 6.0, \text{ and } 10.0$.

The boards with unknown distribution functions were manufactured at Washington State University. These were phenolic-resin bonded flakeboards prepared from douglas-fir (Pseudotsuga menziesii (Mirb.)) flakes having two different aspect ratios (particle length/particle width) 2 and 4. Flakes with an aspect ratio of 4 (.37" x 1.5") were used to prepare boards having 5 levels of orientation, from completely random to the highest orientation obtainable. Flakes with an aspect ratio of 2 (.375" x .75") were used to prepare boards having random and maximum orientation. All flakes were approximately 0.015 inches thick.

Orientation of the flakes was achieved by dropping the particles through an electric field during the mat forming process. The degree

of flake alignment was controlled by varying the electric field from 0 to 6.7 Kv/inch, the higher the electric field, the greater the orientation (Talbot, 1976). The boards were hot pressed for 6 minutes at 375 degrees F. to a thickness of .375 inches, requiring closing pressures from 250 to 300 psi. The final average specific gravity was .67.

A commercial particleboard manufactured by Potlatch Corporation was also used in the study. The board used was a .25 inch thick panel, commercially marketed as the center panel in a plywood-particle board composite. The board consisted of oriented white fir (Abies grandis (Dougl.)) flakes cut at a target thickness of 0.016-0.020 inches, and approximately 1.5 inches in length. The boards were made with 6 percent phenolic resin, and the flakes were oriented to an undetermined degree of orientation by mechanical means. The specific gravity is approximately .62.

Method for Estimating the Concentration Parameter

One major objective of this study was to develop a technique to characterize the orientation of particles in particleboard "in situ". The technique involved making photographic slides of both surfaces of the particleboards initially. A light source was directed from a low angle to obtain the best possible contrast between particles. The slides were projected onto a screen with 50 random points (Figure 4). The points served as sampling locations, and the orientation of the particles at each point was measured to the nearest degree by placing the rotatable straight edge of a drafting machine parallel to the longitudinal (grain) direction and reading the angular deviation from

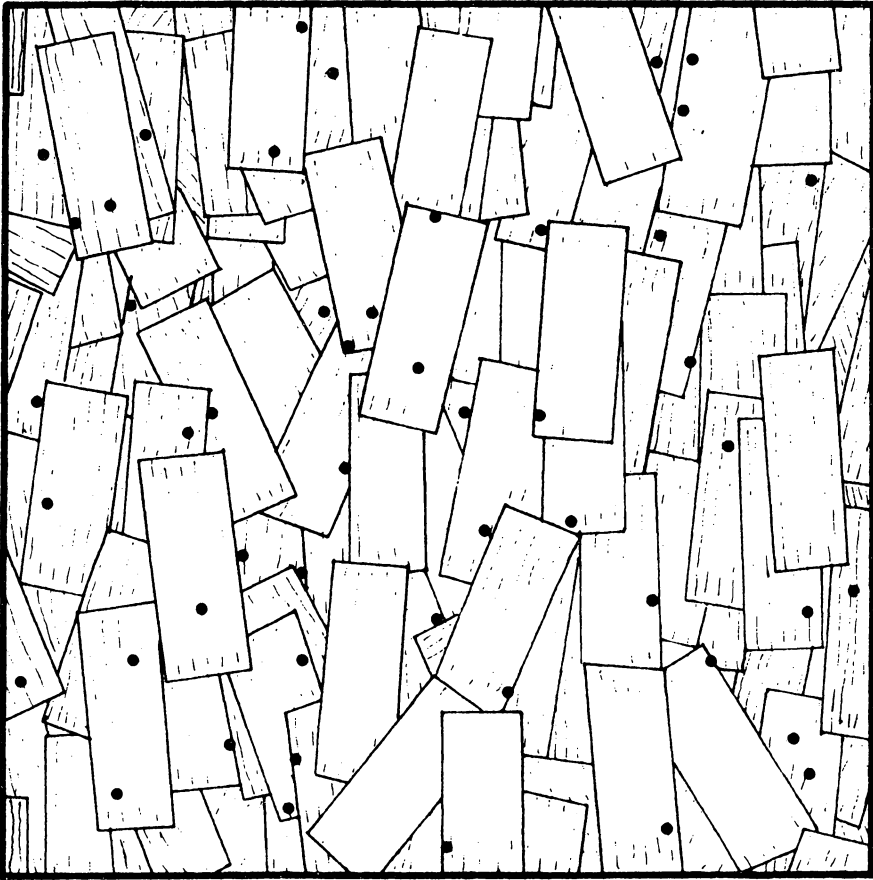


Figure 4. Illustration of sampling method showing fifty random sampling points superimposed on a portion of particle-board.

a scale at the base of the straight edge. Data was collected on both sides of the boards to obtain a comparison of the two sides, yielding a total of 100 points sampled for each board.

After collecting the data, average sines and cosines were calculated. The mean vector, r_o , was determined using Equation 10, and the corresponding concentration parameter, κ , found using the relationship shown in Figure 3.

Simulation of Elastic Properties

Tension

A computer experiment was used to compute an effective elastic modulus of an idealized particleboard strip, Figure 5. The strip was envisioned as a series of wood particle segments of equal lengths with random orientation angles. The stiffness of the segments are replaced with spring constants, k_i , Figure 6a.

$$k_i = \frac{A E_L}{l P_i} \quad (11)$$

where: A is the cross-sectional area of a segment,

l is the segment length,

E_L is the elastic constant in the longitudinal direction,

and P_i is obtained from the transformation of the fourth-order compliance tensor (Jayne, 1972) as given by

$$P_i = \cos^4\theta_i + 2b\cos^2\theta_i\sin^2\theta_i + a\sin^4\theta_i \quad (12)$$

where: θ_i is the deviation of grain angle from axis of strip,

$$a = \frac{E_L}{E_R},$$

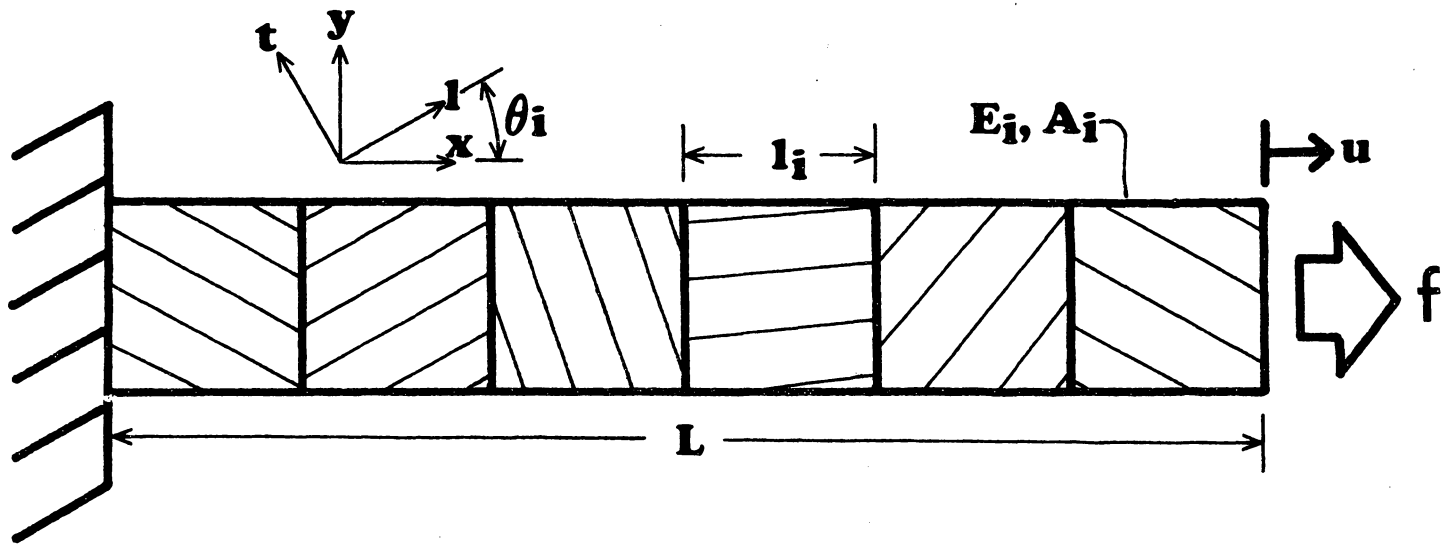


Figure 5. Schematic representation of the strip model.

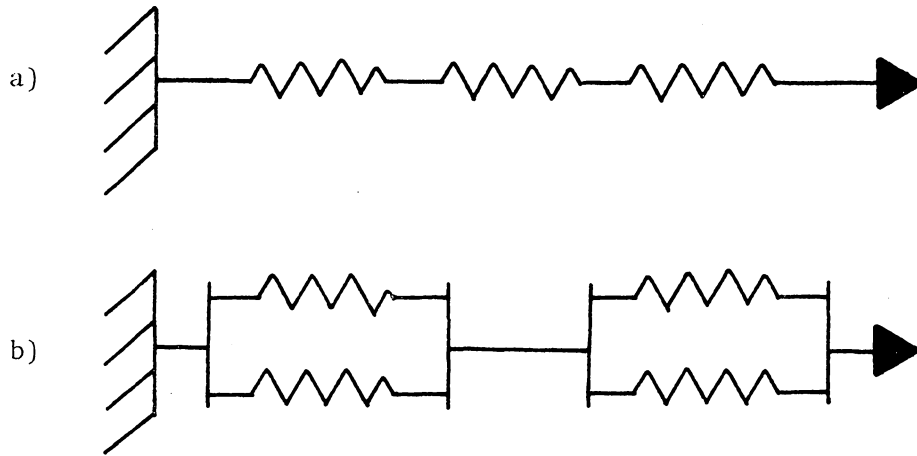


Figure 6. Spring representation of a) unlayered model, and b) layered model.

$$b = \frac{E_L}{2G_{LR}} - \nu_{LR},$$

and E_L , E_R , G_{LR} and ν_{LR} are elastic constants of the wood particles.

It has been shown (Johnson and Harris, 1976) that the effective elastic modulus of the strip is given by

$$E^* = \frac{E_L}{\frac{1}{n} \sum_{i=1}^n P_i} \quad (13)$$

The model assumes a single layer of particles. It can also be modified to account for the effects of layering. If each segment is composed of m layers of particles, each of the same thickness, then the spring constant for each segment is calculated as a stack of parallel spring constants. It can be shown, Johnson and Harris, 1976, that the effective elastic modulus of the layered strip is calculated by Equation 11, with P_i replaced by $\overline{P_i}$, which can be obtained from

$$\frac{1}{\overline{P_i}} = \frac{1}{m} \sum_{j=1}^m \frac{1}{P_{ij}} \quad (14)$$

where P_{ij} is the same expression as Equation 12, with θ_i replaced by θ_{ij} , i.e., the orientation of the j th layer in the i th segment. Thus, the layered model can be thought of as a set of segments in series, where each segment is made up of a set of spring in parallel shown skematically in Figure 6b.

Four species were used in the study, and they are listed in Table 1, along with their respective elastic constants which were used in the

Table 1. Elastic constants used in simulation models (Wood Handbook, 1974, Bodig and Goodman, 1975).

Species	Young's Modulus ¹		Shear Modulus ¹	Poisson's Ratio	Specific Gravity ²
	E_L	E_R	G_{LR}	ν_{LR}	g
<i>Pinus strobus</i>	8280	676	580	0.37	0.35
<i>Populus tremuloides</i>	8750	724	586	0.48	0.36
<i>Pseudotsuga menziesii</i>	15700	1060	882	0.20	0.48
<i>Abies grandis</i>	12700	931	931	0.30	0.37

¹ Units in MPa

² Oven-dry weight/green volume

models. The elastic parameters are from the Wood Handbook, 1974 and Bodig and Goodman, 1975.

Shear

The shear model used to determine the theoretical effects of orientation on the shear modulus of particleboard consisted of a square mini-panel made up of square particles. The mini-panel represents an attempt to simulate a portion of a particleboard panel, Figure 7. This type of system lends itself to finite element analysis in which the particles can be modeled as elements, or a collection of elements. The edges of the mini-panel are displaced into a shape of pure shear strain, γ , as shown in Figure 7. The interior edges were not constrained in this model. Since the finite element program calculated the work done on the system (or alternatively, the potential energy of the system, ϕ) and since a state of pure shear strain, γ , was superimposed on the edges of the mini-plate, a definition of an effective shear modulus for the mini-plate was developed based on these two variables:

$$G^* = \frac{2\phi}{\gamma^2 V} \quad (15)$$

where V is the volume of the mini-panel. In this way, the uneven distributions of both the shear and normal stress components within the mini-panel could be ignored. Although this is only one possible definition of an effective shear modulus, it was felt that it was adequate for the objectives of this study. A complete understanding of the heterogeneous nature of the model was beyond the scope of this study.

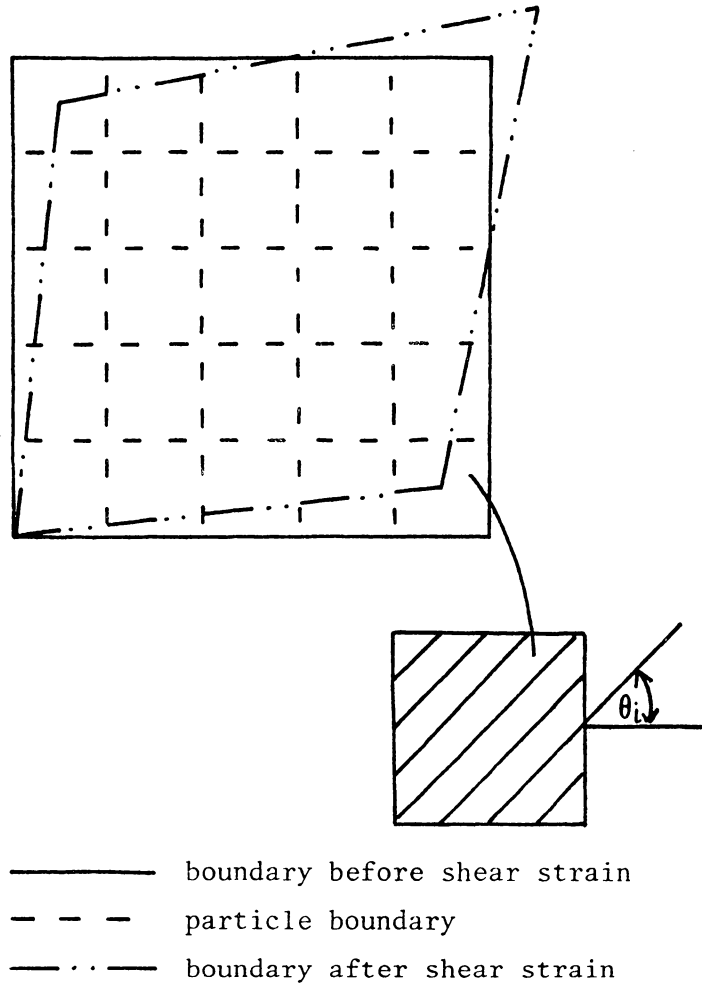


Figure 7. Schematic representation of shear model.

The finite element program used in the shear modulus analysis was a modified version of the program used by Johnson, 1973.

Experimental Measurements

The mechanical properties selected for evaluation in this study were the tensile elastic modulus, plate shear modulus, poisson's ratio, modulus of elasticity, and modulus of rupture.

Specimens for the tensile elastic modulus determination were cut one inch wide. The longitudinal axis of the specimens were parallel to the principal board direction. Four tension specimens were cut from each board with known distributions, twelve from each level of orientation in the WSU boards, and five from the Potlatch board.

A floor model Instron was used to test the samples. An extensometer with a gauge length of 25.4 mm (1") was used to monitor displacement and a crosshead speed of .02 mm/sec. (.05 in/min.) was employed. An elastic modulus for each sample was calculated using the slope of the greatest linear portion of the force/deflection (stress/strain) diagrams.

The ASTM panel shear test was evaluated for use in the study, however, the size of the specimens as well as the difficulty in performing the tests appeared prohibitive. An alternative was sought, and the plate shear test appeared to be the best.

A preliminary test was run to determine if the plate shear method was comparable to the ASTM panel shear test. The limited data indicates that the plate shear and panel shear tests are quite comparable. The experimental results are:

		<u>MPa</u>	<u>ksi</u>
Plate Shear:	Mean	1379	200
	Standard Deviation	159	23
Panel Shear:	Mean	1524	221
	Standard Deviation	165	24

Thus, the ASTM Standard D 3044-72 plate shear test was used to determine the shear moduli of the particleboards used in this study. This method is associated with the measurement of the in-plane shear modulus of the particleboard. The ASTM Standard specifies that the plate shear test specimen be square, with the thickness equal to the thickness of the material, and the side dimension not less than 25 nor more than 40 times the thickness. To comply with this requirement, the following edge lengths were used: 6 inches for the boards of known distribution; 11 inches for the WSU and Potlatch boards.

The tests were performed on a table model Instron, using a head speed of .5 cm/minute. The shear modulus for each sample was calculated using the slope of the linear portion of the force/deflection (stress/strain) diagram.

Poisson's ratio was determined for the WSU boards. Test samples examples like those used for the tensile tests were used for the Poisson's ratio. Testing was carried out on an Instron testing machine equipped with an extensometer to determine the longitudinal extension. The lateral contraction was measured by a linear differential variable transformer, and Poisson's ratio, ν , was calculated as the ratio of the

longitudinal extension to the lateral contraction.

One inch wide test strips were cut from the WSU and Potlatch sample boards to determine MOE and MOR in the plane of the board. Twelve WSU specimens were used for each level of orientation, and five specimens were prepared from the Potlatch material. ASTM Standard D 1037 was used to determine the MOE and MOR in bending. A span of 9 inches was used for the WSU strips and a span of 6 inches was used for the Potlatch specimens.

The tests were performed on a table model Instron, using a head speed of .5 cm/minute. The MOE was calculated from the slope of the linear portion of the force/deflection (stress/strain) diagrams.

RESULTS AND DISCUSSION

This section is divided into four major areas: (1) characterization of orientation, (2) simulation results, (3) experimental results and (4) a comparison between theory and experiment.

A specific technique to determine and characterize the orientation of particles in particleboard "in situ" is discussed first, followed by an assessment of the technique. The effects of orientation on the mechanical properties of particleboard is presented in a two-step manner. The first step involves determining theoretical results by modeling; the second involves the actual testing of experimental boards with various degrees of orientation. A final phase compares the theoretical and experimental results.

Characterizing Orientation

A primary objective of this phase of the study was to estimate the state of orientation in particleboard. It was felt that a match between the measured parameters of systems with known degrees of orientation and the actual parameters used to manufacture these systems would determine the effectiveness of the measuring technique.

Particle orientation was measured on particleboards with known distribution functions by the method previously outlined, which consisted of sampling particle angles at various points on the particleboard surface and calculating the mean vector, r_o , and the concentration parameter, κ .

The raw data consisted of a collection of angles with a range of 0 to π (0 to 180 degrees). Each angle was doubled to obtain a range of

0 to 2π (0 to 360 degrees). The results of measurements on the five groups of manufactured boards are presented in Figure 8 in the form of circular histograms. The values of κ are those used to manufacture the boards. The frequency of measurements within 10° intervals is represented by different dot sizes. The largest of the four dot sizes represents four measurements; the smallest, one. It is clear that the distributions tend to cluster about the mean direction as the concentration parameter increases. A measure of this clustering is provided by the length of the mean vector, r_o , which was calculated according to Equation 10 after doubling the angles.

The estimated and known orientation concentration parameters, as well as the length of the mean vectors are shown as follows:

<u>r_o</u>	<u>Calibrated</u> <u>κ</u>	<u>Estimated</u> <u>κ</u>
0.056	0.03	0.11
0.403	0.90	0.88
0.766	2.50	2.51
0.893	5.00	4.99
0.960	50.50	12.80

The estimated and known values of the concentration parameter are in reasonable agreement, indeed, a paired comparison using a t-test reveals no significant difference between the calibrated and estimated values at the 5 percent confidence level ($t(\text{calc}) = 0.996$ $t(0.5,4) = 2.78$). A large discrepancy does occur in the highest orientation measurement, however, this should not be viewed with alarm. As seen

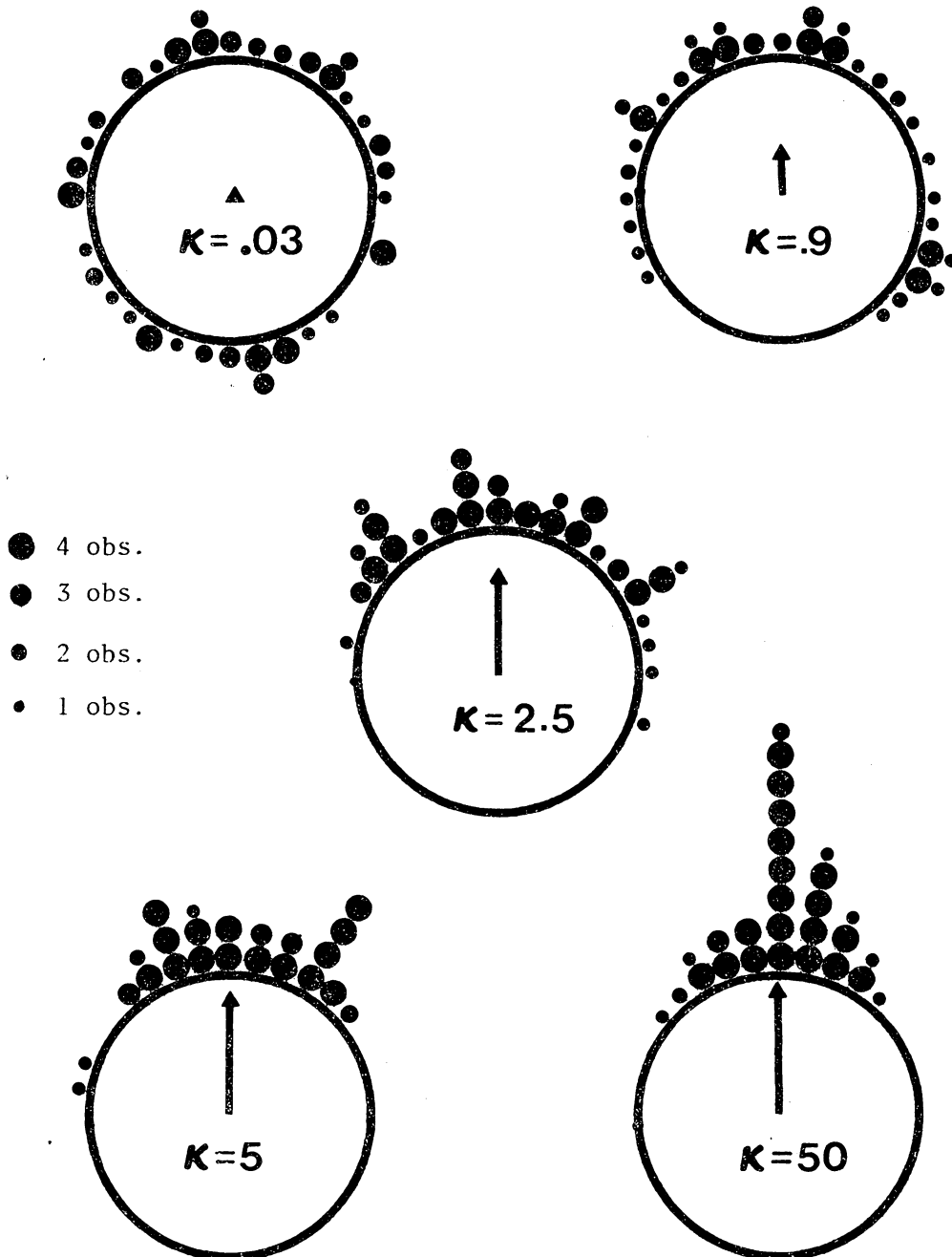


Figure 8. Circular histograms showing the degree of orientation of the experimental boards (the measured angles were doubled).

in Figure 3, the slope of the curve depicting the relationship between the mean vector and the concentration parameter is quite steep when the length of the mean vector is greater than 0.90. Thus, in actuality, there is little difference in the distribution functions when $\kappa = 50.5$ and $\kappa = 12.8$.

This close comparison between the known and estimated concentration parameters indicates that the sampling techniques developed is quite consistent, and can be used to measure the degree of orientation of particles in particleboard.

Orientation of the WSU and Potlatch boards were also determined. The WSU boards (a total of 42 boards) were sampled on each side with over 5500 individual particle angles recorded. Average mean vectors were calculated, and the corresponding κ determined. For the five board groups with aspect ratios of 4, the κ 's were: 0.193, 0.279, 0.767, 1.759, and 2.587. For the two board groups with aspect ratios of 2, the κ 's were 0.104 and 2.395.

An analysis of variance of the mean vectors (arranged in groups of 10 to provide an error term) showed that there was no difference in the mean vector between the two sides of the boards, no difference between boards within a single orientation group, but a significant difference between orientation groups. The results of the ANOVA are as follows.

<u>Source</u>	<u>df</u>	<u>Mean Square</u>	<u>Prob. > F</u>
Sample	6	4.084	0.0001**
Board (Sample)	35	0.033	0.1188
Side (Sample Board)	42	0.023	0.2105
Residual	437	0.020	

Angles were similarly measured on the Potlatch boards, and r_0 and κ were determined to be 0.6621 and 1.800, respectively. This was a result of nearly 600 individual measurements on the Potlatch boards.

During the investigation it was observed that orientation up to approximately $\kappa = 1$ is not noticeable to the observer. In the range $1 < \kappa < 2$, the particles are noticeably oriented in a preferred direction. Above $\kappa = 2$, the orientation is quite obvious, Figure 1. The author was quite often asked by persons looking at the Potlatch boards ($\kappa = 1.8$), "are these particles really oriented?" From these casual observations, and from the estimated concentration parameters of the WSU and Potlatch boards, it would appear that neither the electrostatic nor the mechanical aligning method used in the manufacture of these boards orients the particles to the maximum orientation possible. Thus, the processes now available for aligning particles must be greatly refined before the potential benefits of orientation can be realized.

Results of Model Simulations

Tension

Calculations for the effective elastic modulus of an unlayered strip were made using Equation 13. The axial direction of the strip was assumed to be parallel to the preferred direction of the orientation distribution function. Preliminary calculations indicated that the number of segments in the strip did not have a great effect on the average effective modulus. The model used consisted of six segments (or particles) for each strip and twenty strips were used at each level of orientation. The resulting twenty elastic moduli were averaged, and a standard deviation calculated. The average elastic modulus increased

with an increasing orientation, Figure 9.

It is interesting to note that the elastic modulus increased nearly seven-fold from a random to a highly oriented system. This points out the profound difference particle orientation can have on the stiffness of particleboard.

As the orientation increases, one would expect the standard deviation to decrease, due to the tendency for the angles to cluster more tightly around the mean at the higher degree of orientation. However, the standard deviation passes through a maximum and decreases only at very high orientations, Figure 10.

The large standard deviations in the middle orientation range can be explained by the occasional occurrence of an angle which deviates greatly from the mean. This acts as a flexible link, reducing the stiffness of the strip and causing a large deviation between the strips. At lower levels of orientation, all strips are flexible, and at higher orientations, all strips are stiff, thereby reducing the standard deviation.

The model was also modified to include the effects of layering on the stiffness of boards with aligned particles. Models consisting of six segments, each segment being made up of six layers, were used. Again, twenty strips were calculated for each level of orientation.

In the non-layered model, any segment with the longitudinal direction perpendicular to the axial direction of the strip will act as a flexible link and thus reduce the overall stiffness. In the layered model, however, the probability of all layers within a segment being perpendicular to the axial direction is small, even at lower levels of

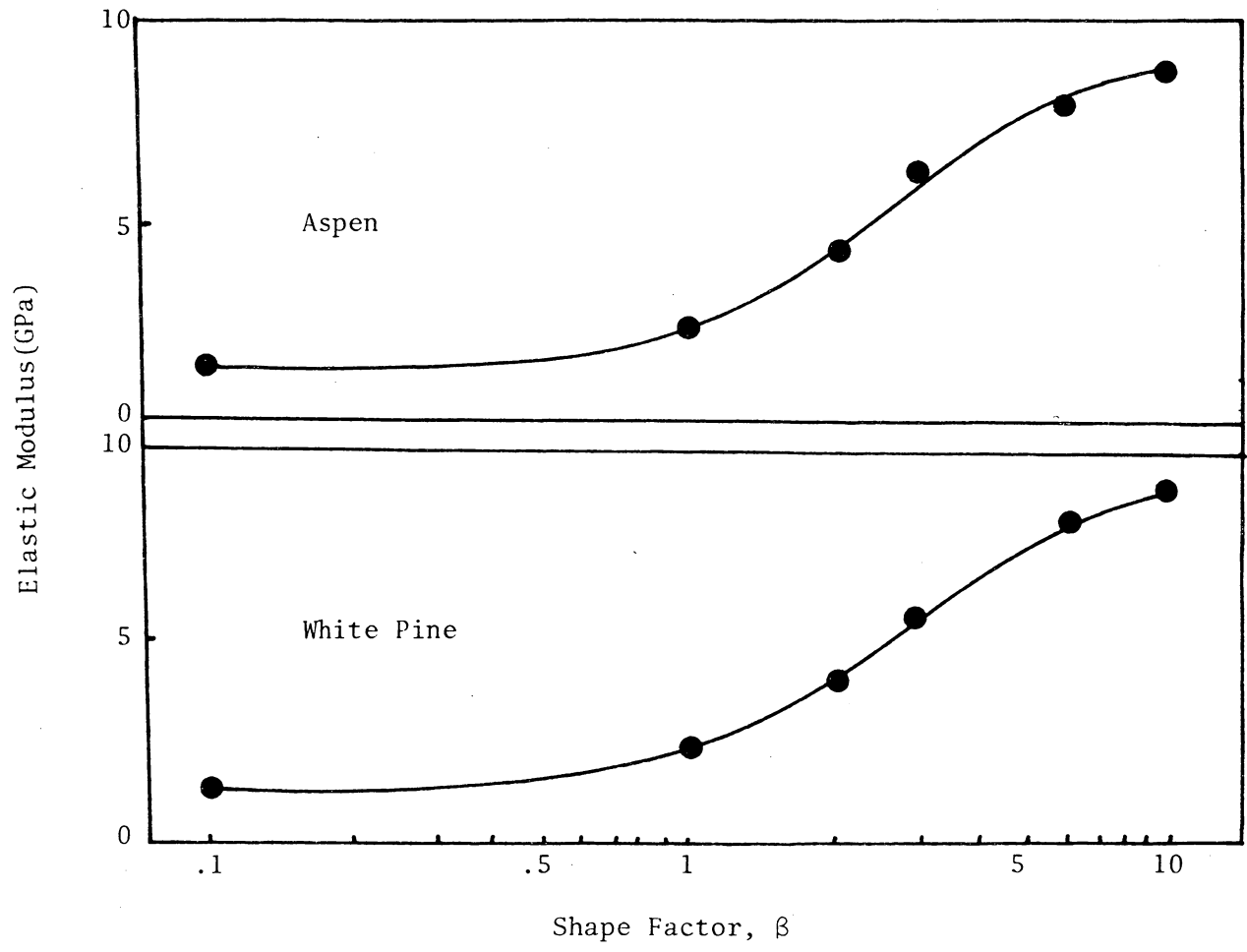


Figure 9. Tensile elastic modulus of white pine and aspen as a function of the degree of orientation.

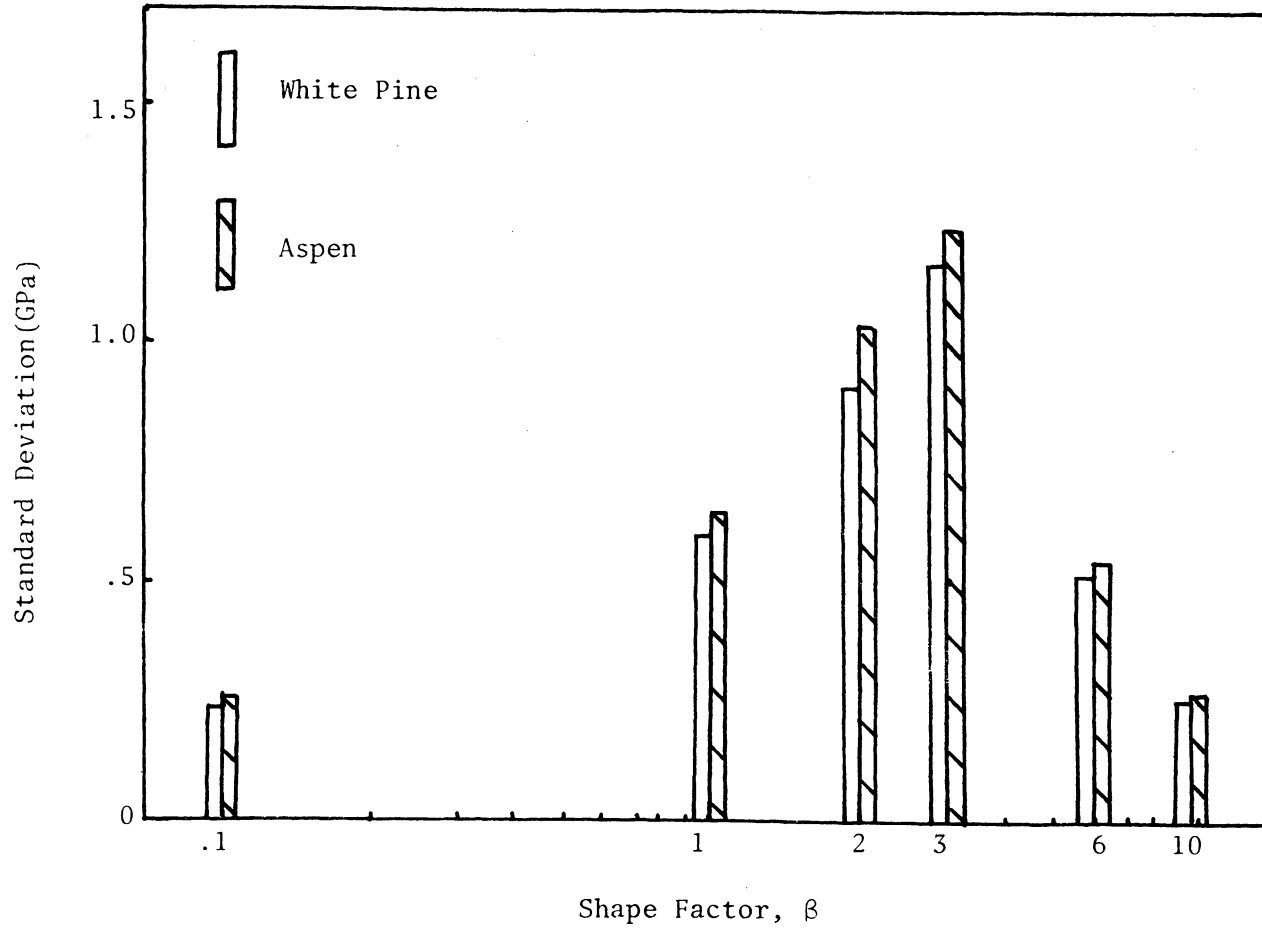


Figure 10. Standard deviations of white pine and aspen tensile elastic modulus as a function of the degree of orientation.

orientation and consequently the overall average stiffness is elevated, Figure 11.

As the probability of a segment with a high angular deviation from the principal board direction is reduced (i.e., at higher β 's), the effects of layering are reduced. Therefore, layering the model resulted in a greater elastic modulus at low values of β , and little change at high values of β , when compared to a non-layered model, Figure 11. For example, the effective elastic modulus of the layered model at $\beta = 1$ is approximately 100 percent greater than the unlayered model for both species.

Layering also had the effect of reducing the standard deviation, although the maximum standard deviation still occurs in the middle orientation range.

	0.1	1.0	2.0	3.0	6.0	10.0
St. Dev. (Wt. Pine, MPa)	359	496	331	276	103	76
St. Dev. (Aspen, MPa)	379	524	352	290	103	76

The layered model was used to project estimated elastic moduli for the WSU and Potlatch boards. Since the specific orientation of these boards were not known, the shape factors for each level of orientation were estimated using the procedure previously discussed. These estimated shape factors were then used to generate angles to be used in the model, according to Equation 8.

The estimated values for the USE boards, along with the standard deviations, are:

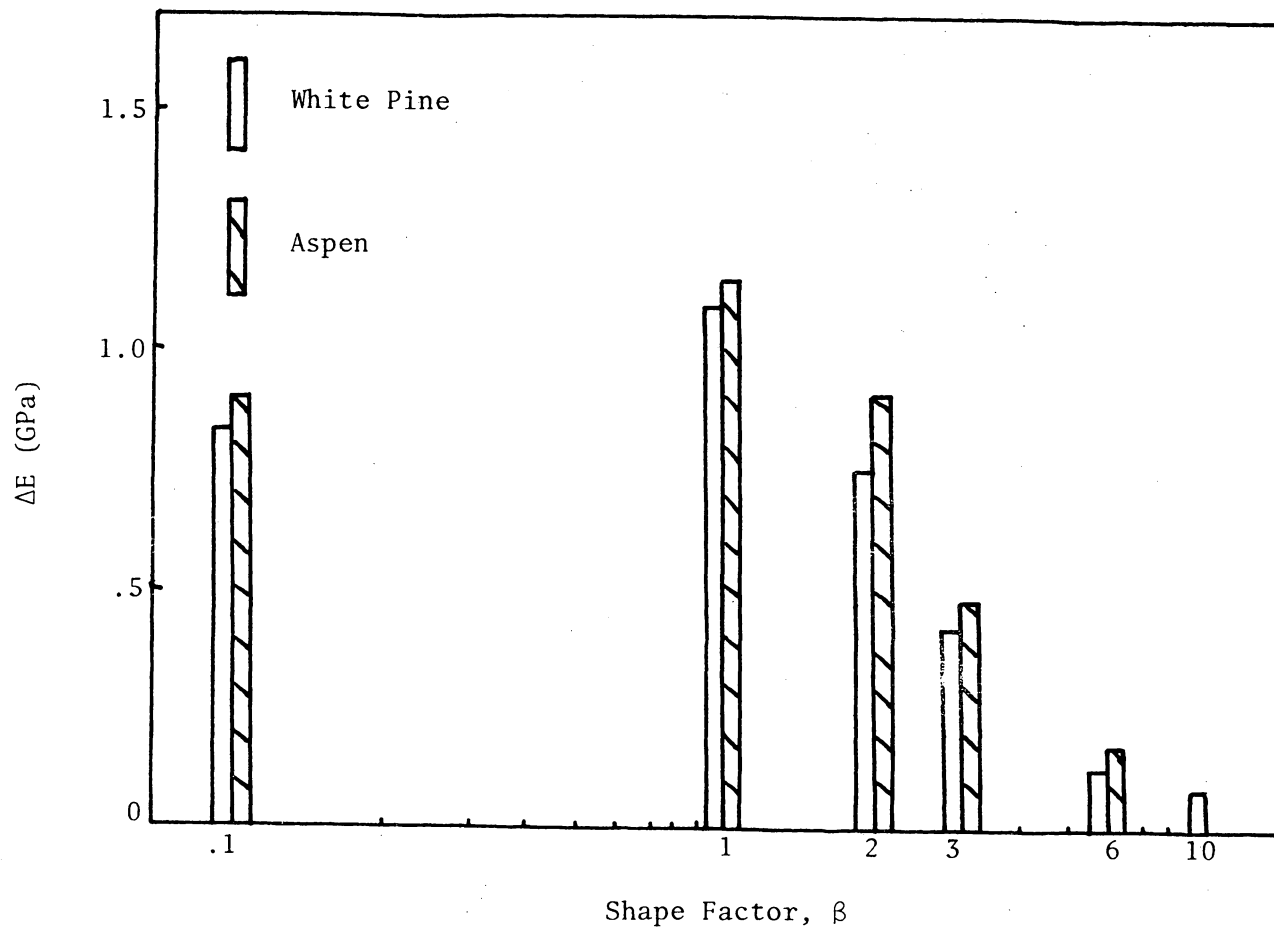


Figure 11. Difference between the effective elastic modulus of the layered and unlayered models, $E_L - E_{UL} = \Delta E$.

β	0.31	0.44	0.54	0.94	1.59	1.95	2.04
E*(MPa)	3309	3723	4137	5516	7377	8618	8687
St. Dev. (MPa)	662	758	758	827	827	896	827

The Potlatch boards had an estimated elastic modulus of 9360 MPa. This was based on a shape factor of $\beta = 1.61$.

These results indicate that the tensile elastic modulus increases greatly in the direction of particle alignment as the degree of particle alignment increases. The standard deviation increases to a maximum at moderate levels of orientation, and decreases at higher levels of orientation.

Shear

A preliminary study was made with the shear model to determine the effects of the element size in relation to the particle size on the shear modulus. It was felt that if the grain angles of adjacent particles were perpendicular to each other, the model would show the most erratic pattern of shear stress distribution. Therefore, the model used consisted of a mini-panel of four particles. The grain angle of the lower left and upper right particles was 45 degrees, and the grain angle of the upper left and lower right particles was -45 degrees, Figure 12a. Three computer runs were made: (1) the particle and element size equal (4 elements total), (2) each particle consisting of four elements (16 elements total), and (3) each particle consisting of nine elements (36 elements total), Figure 12b.

This shear model revealed that the shear stress, τ_{xy} , along the

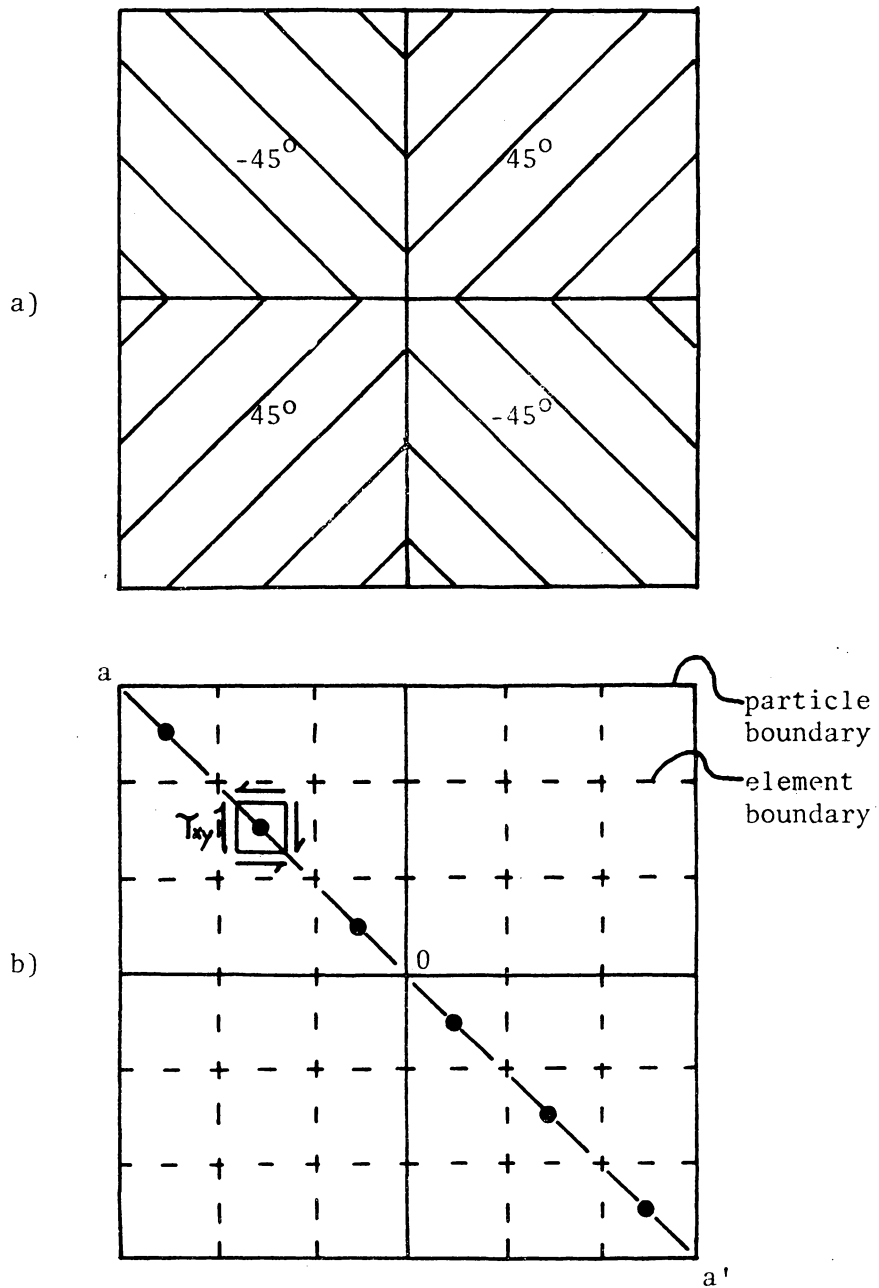


Figure 12. Plate shear model, with a) the element size equal to the particle size, and b) the particles divided into nine elements.

diagonal, a-a', was not constant, but increased to a maximum in the center of the mini-panel as shown in Figure 13. Thus, the assumption of a state of pure shear stress throughout the mini-panel is not valid. Figure 14, however, reveals that the case in which the element size is equal to the particle size represents an approximate average across the diagonal. Thus, although these are constraints at particle boundaries that prevent a state of pure shear within the particles, it was felt that a one particle-one element model represented an average gross behavior of the mini-panel.

Another possible problem was the effect of the total number of particles comprising the mini-panel on the shear modulus. Five systems of elements (total number of elements were 4, 16, 36, 100 and 144) and two shape factors ($\beta = 0.1$ and 6.0) were tested to determine the effects of the particle size. A state of pure shear was imposed on the boundary of the mini-panel, and the resulting potential energy (the average of 5 runs) is shown in Figure 10, which indicates that the shear modulus as calculated with Equation 15 would remain constant after the total number of elements reaches 16. As a consequence, a model consisting of 36 elements (6 x 6) was used in the remainder of the study.

During the analysis of the preliminary simulations, it was observed that the stress distribution in the panels of uniform random orientation were quite variable as compared to the distribution of the stresses in the highly oriented system, Figure 15. A first impression was that there might be a correlation between the particle angle and the stress concentrated in that particle, however, a correlation analysis between

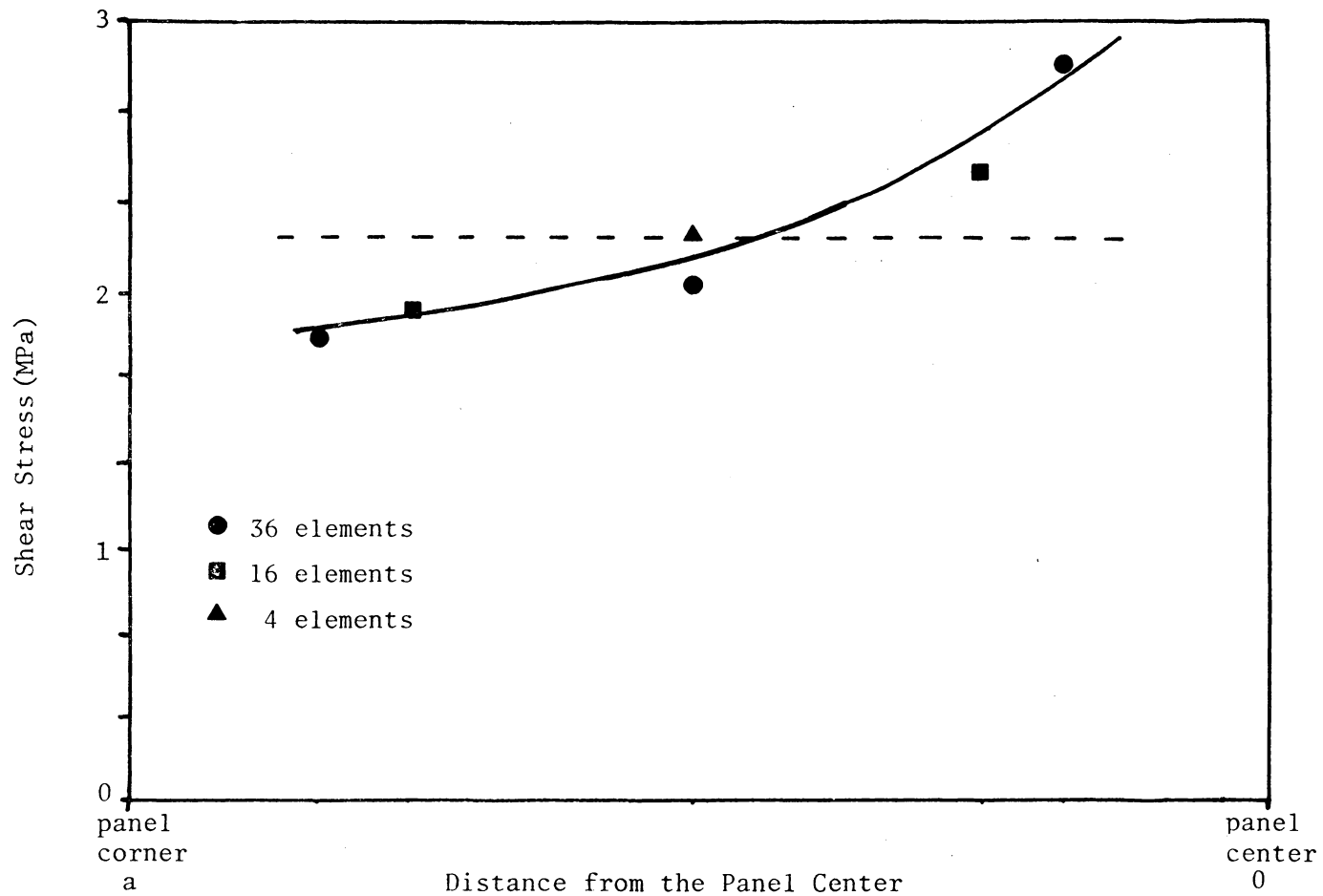


Figure 13. Shear stresses present along the panel diagonal for various element sizes.

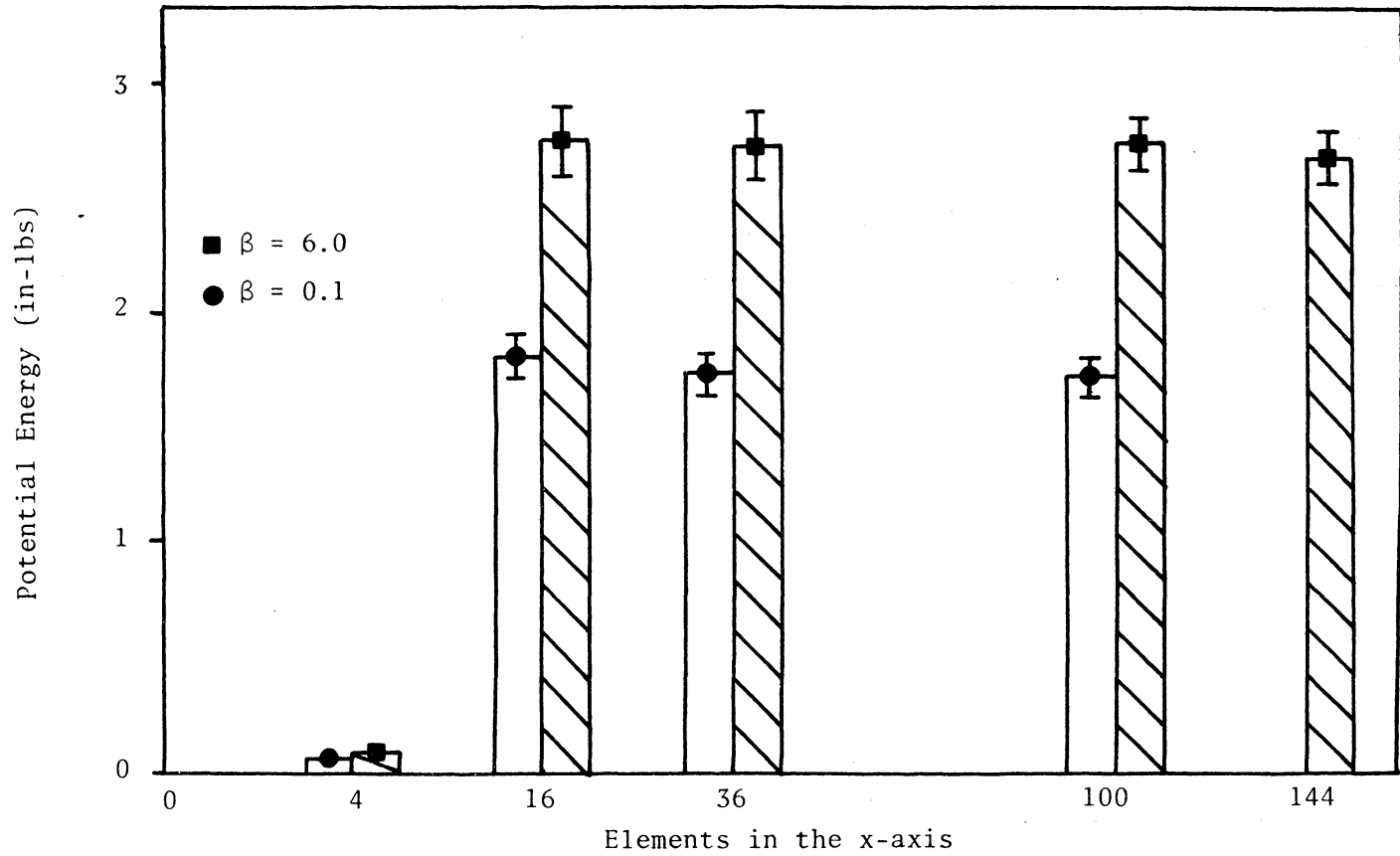


Figure 14. Potential energy as a function of the number of elements in the shear model.

136 57	121 -13	87 45	128 11	226 -77	142 87
201 -53	95 -45	122 76	209 -84	75 -24	83 -67
76 -82	132 -67	211 -16	112 17	104 73	123 47
136 63	141 57	112 71	120 -79	183 -80	104 -45
107 59	106 24	79 -50	175 -36	116 61	82 5
101 36	70 -76	164 25	111 -35	81 34	146 -33

 $\beta = 0.1$ Shear Stress (ksi)
Angle (degrees)

84 6	85 -1	87 5	85 1	86 -10	89 15
90 -6	89 -5	84 10	84 -13	78 -2	83 -8
88 -12	89 -8	87 -2	84 2	87 9	87 5
86 7	90 6	90 8	88 -11	86 -11	83 -5
92 6	82 2	84 -5	95 -4	90 7	84 1
87 4	86 -10	89 2	86 -3	88 3	93 -3

 $\beta = 10$

Figure 15. Shear stress distribution in elements of shear model for two betas.

shear stress and orientation angle within an element showed an r-square of less than 0.1. The difference in the stress distributions must be a complex result of interactions between neighboring particles with varying angles, causing the uniform randomly oriented boards to have an increased deviation in stress distributions from particle to particle. This could prove to be an important factor in the reliability of particulate panels and is an area to which further research should be devoted.

The response of the shear modulus to orientation is the reverse of the response of the tension modulus, that is, as the degree of orientation increases, the shear modulus decreases, Figure 16. The shear modulus, however, is less severely affected than the tensile modulus, with a decrease of less than 50 percent from highly oriented to uniform random.

The standard deviation of the shear simulation is small, and unlike the standard deviation of the tension model which passes through a maximum, the standard deviation of the shear modulus decreases as the orientation increases.

β	0.1	1.0	2.0	3.0	6.0	10.0
St. Dev. (Wt. Pine, MPa)	55	48	41	21	14	7
St. Dev. (Aspen, MPa)	55	48	41	21	14	7

This indicates that orientations within individual particles are not as critical in determining the shear modulus as they are in the tensile strip models.

The estimated shape factors were used in the finite element model to predict the shear modulus for the WSU and Potlatch boards. The

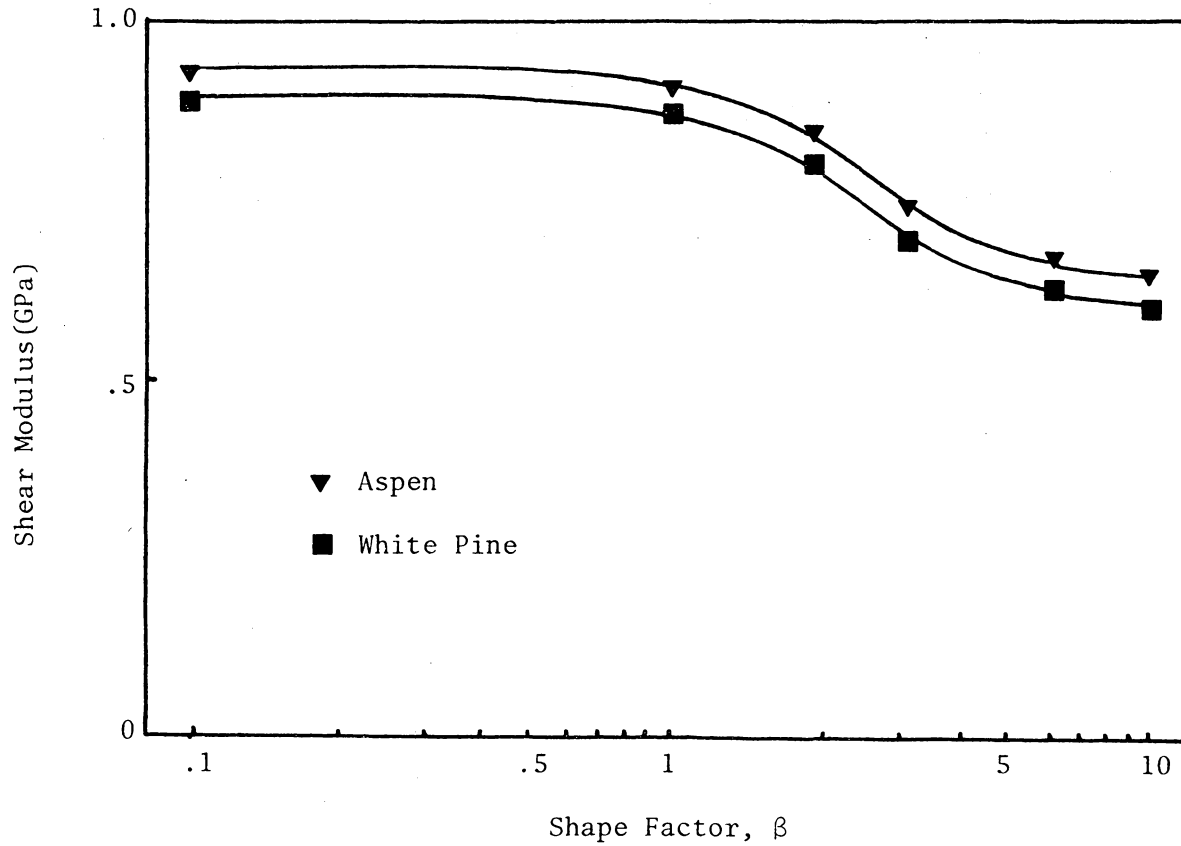


Figure 16. Shear Modulus of white pine and aspen as a function of the degree of orientation.

WSU results were:

β	0.31	0.44	0.54	0.94	1.59	1.95	2.04
G (MPa)	779	958	883	876	834	676	676
St. Dev. (MPa)	110	110	165	165	214	55	152

The Potlatch board, with a shape factor, $\beta = 1.61$ had a predicted shear modulus of 1034 MPa.

Experimental Results

The experimental results are presented briefly in this section, and discussed further in the following section which compares them with the simulation results.

Boards with known distribution functions

As previously indicated, the tensile elastic modulus was measured on a floor model Instron equipped with an extensometer to measure the longitudinal extension. The raw data is presented in Appendix A (Tables A-1 and A-2). The average tensile elastic modulus is plotted in Figure 17 as a function of the shape factor, β . As shown in Figure 17, the tensile elastic modulus increases with an increasing orientation. As the shape factor goes from 0.1 to 10, the elastic modulus nearly tripled.

The shear modulus decreased as the orientation increased. The shear modulus at a shape factor of 10 showed a reduction of approximately 50 percent compared with the shear modulus at a shape factor of 0.1.

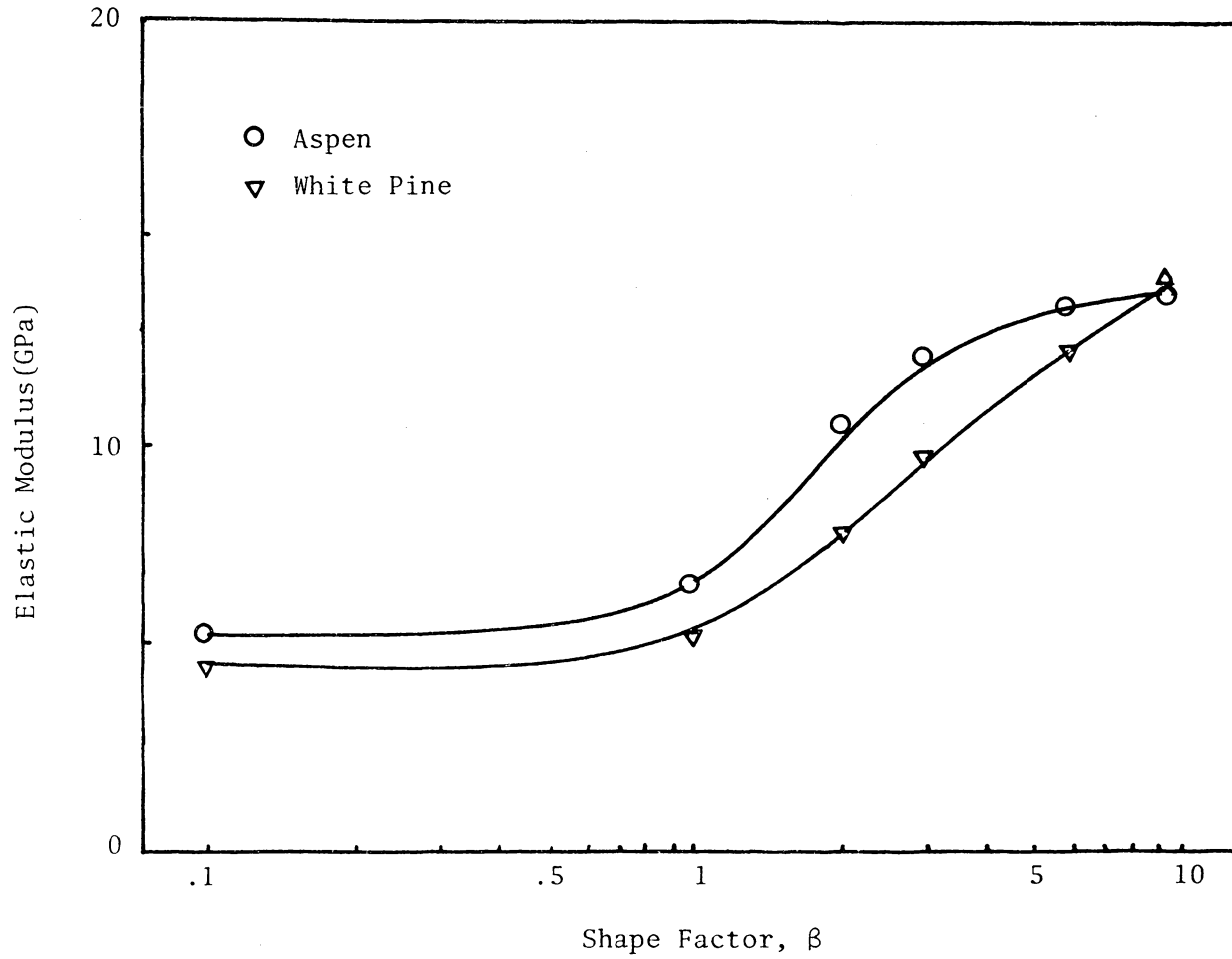


Figure 17. Experimental tensile elastic modulus for white pine and aspen as a function of the degree of orientation.

β	0.1	1.0	2.0	3.0	6.0	10.0
G (Wt. Pine, MPa)	2020	1917	1172	979	972	903
St. Dev.	496	738	248	207	48	255
G (Aspen, MPa)	1993	1848	1565	1358	1227	1172
St. Dev.	69	76	69	138	14	90

A much larger standard deviation is noted for the white pine samples. This is probably a result of not pressing the white pine boards during cooling, causing a slight warping of some of the boards. The aspen boards, the second set made, were pressed during cooling and this resulted in a more uniform end product.

Boards with unknown distribution functions

The tensile elastic modulus and shear modulus of the WSU boards are summarized in Table 2 (raw data appears in Appendix A, Tables A-3 and A-4). As with the white pine and aspen boards, the tensile elastic modulus increased and the shear modulus decreased as the particle alignment increased.

Poisson's ratio

Experimental tests were run on the WSU boards to determine if Poisson's ratio is affected by particle orientation. Based on the limited scope of this study, it appears that Poisson's ratio increases as the degree of orientation increases, Figure 18. This finding was expected since solid wood has a much higher ν_{LR} than ν_{RL} , and as the orientation increases, the particle board more closely resembles solid wood aligned in the direction of orientation.

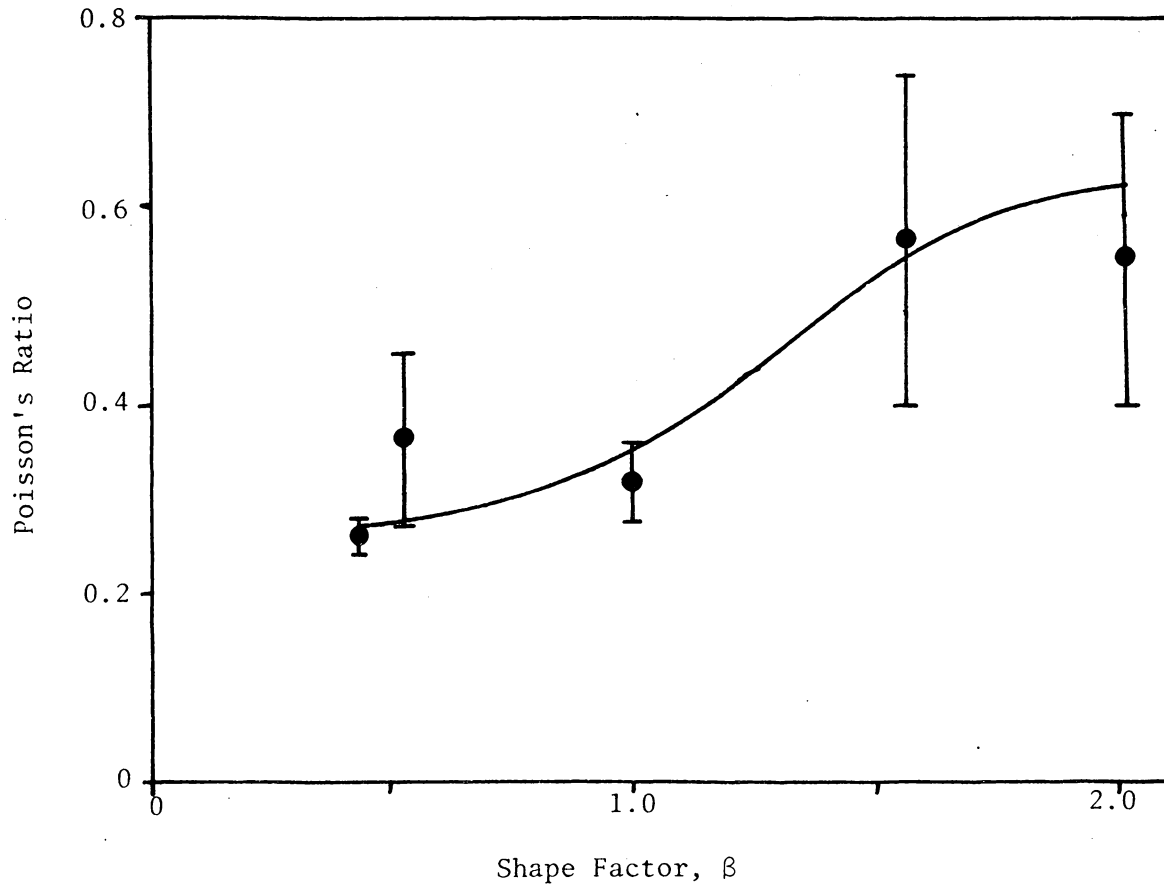


Figure 18. Poisson's ratio of WSU boards as a function of degree of orientation.

MOE and MOR

Both modulus of elasticity, MOE, and modulus of rupture, MOR, in bending were determined for the WSU boards. The results, summarized in Appendix A (Tables A-5 and A-6), are shown graphically, along with regression lines, in Figure 19 and 20, as a function of orientation.

As the orientation increases, both MOE and MOR increase in the direction of orientation. In the range tested ($\beta = 0.31$ to 2.04), both MOE and MOR were approximately doubled. This indicates the practical advantage of orienting particles in particleboard. By doubling the stiffness and strength, the amount of raw material as well as the weight of the finished product is reduced for a board designed for a specific load-bearing capacity.

Effects of particle length

A set of highly oriented boards and a set of randomly oriented boards were constructed at WSU with particle lengths of .75 inches, compared to the other sample boards whose particle lengths were 1.50 inches. The purpose was to determine the effect of particle length on various mechanical properties of the boards. The results of an analysis of variance test to determine the effects of particle length are given in Appendix B. The ANOVA indicates that in this study, particle length had no effect on the tensile modulus, shear modulus, MOE or MOR.

Potlatch boards

The results of the experimental testing of the Potlatch boards are: Tensile elastic modulus - 9398 MPa, and shear modulus - 2496 MPa.

Since only one level of orientation was available for the Potlatch

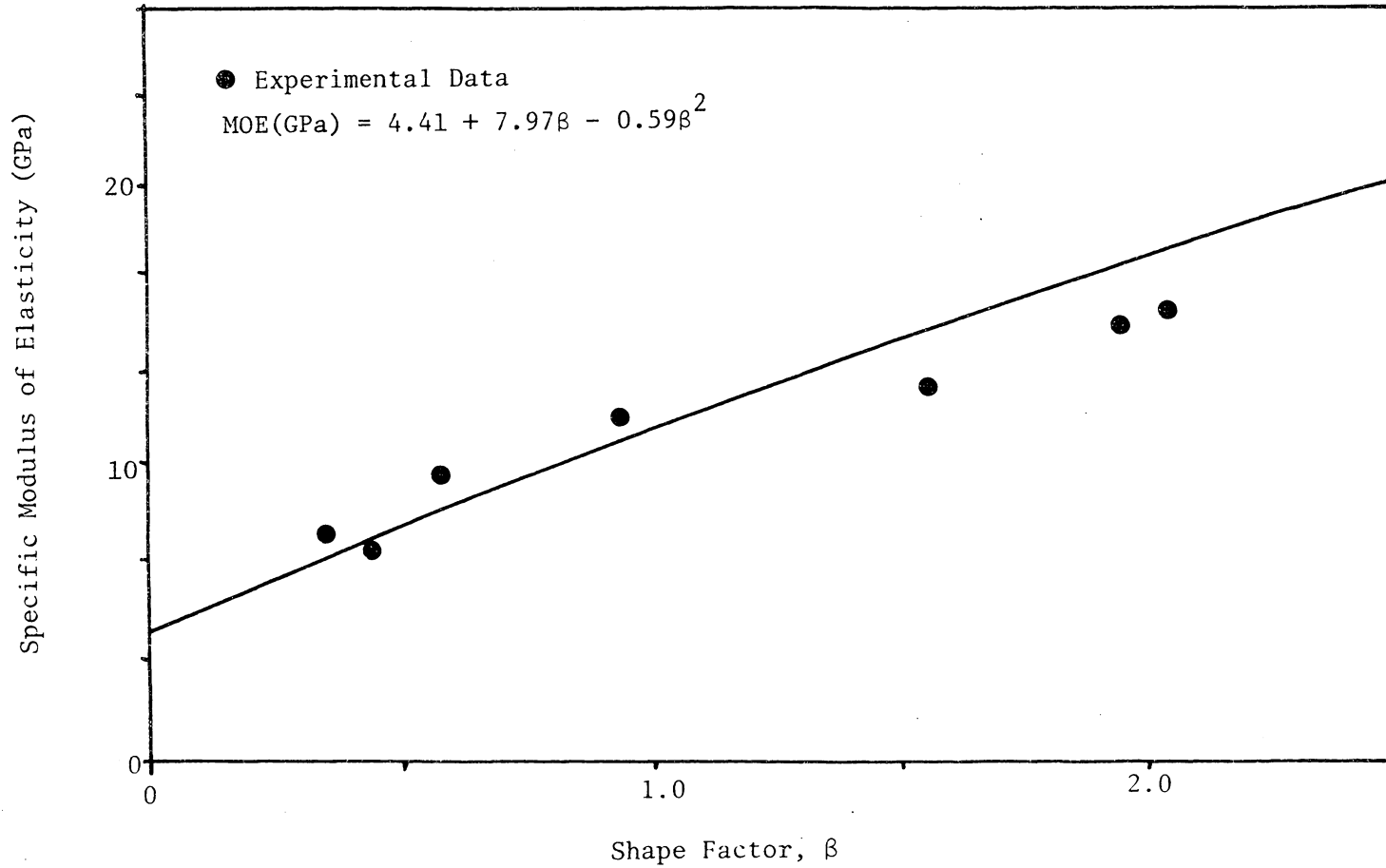


Figure 19. MOE for WSU boards as a function of the degree of orientation.

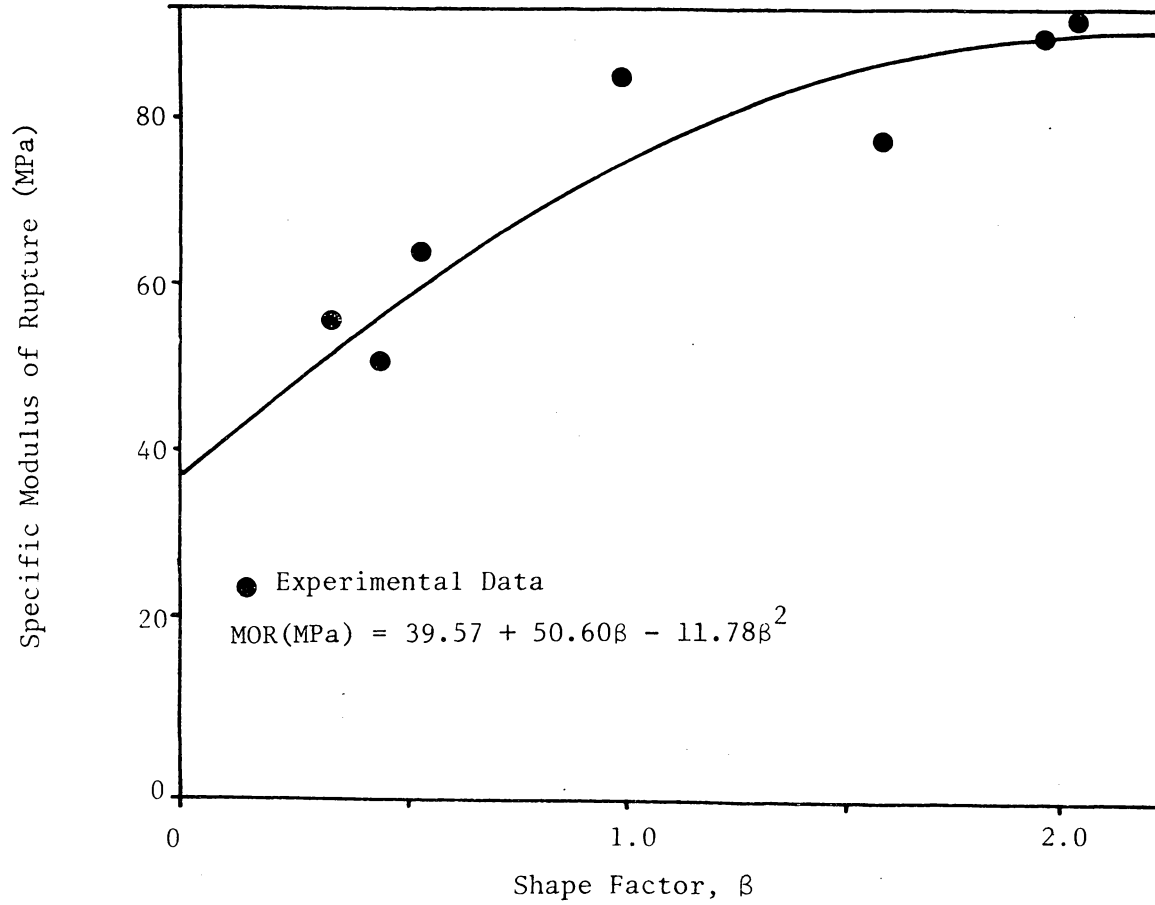


Figure 20. MOR for WSU boards as a function of the degree of orientation.

boards, no statements can be made regarding the effects of orientation on this board.

Comparisons Between Theory and Experiment

Tension

A graphical comparison of the unlayered tensile model and the experimental tensile modulus of the boards with known orientations is given in Figures 21 and 22. Both experimental and theoretical results indicate a similar increase in elastic modulus, however, the model produces much lower values. There are probably two reasons for the divergence between theory and experiment. The first is the densification of the particleboard due to pressing and the addition of adhesive and the second is due to restraints caused by layering. The raw material used for the flakes, white pine, and aspen have specific gravities of approximately .35, and .36, respectively, and the stiffness values used in the theoretical model are based on this density. The finished boards, however, have specific gravities (oven dry weight, oven dry volume) of approximately .63. Assuming the effective elastic modulus is proportional to density, the effect of density can be accounted for by plotting the specific elastic modulus which is the modulus divided by specific gravity, g (oven dry weight, green volume basis).

$$E_s^* = E^* / g$$

$$G_s^* = G^* / g$$

The second reason that the model produces lower values could be due to the effects of layering. As previously discussed, layering the

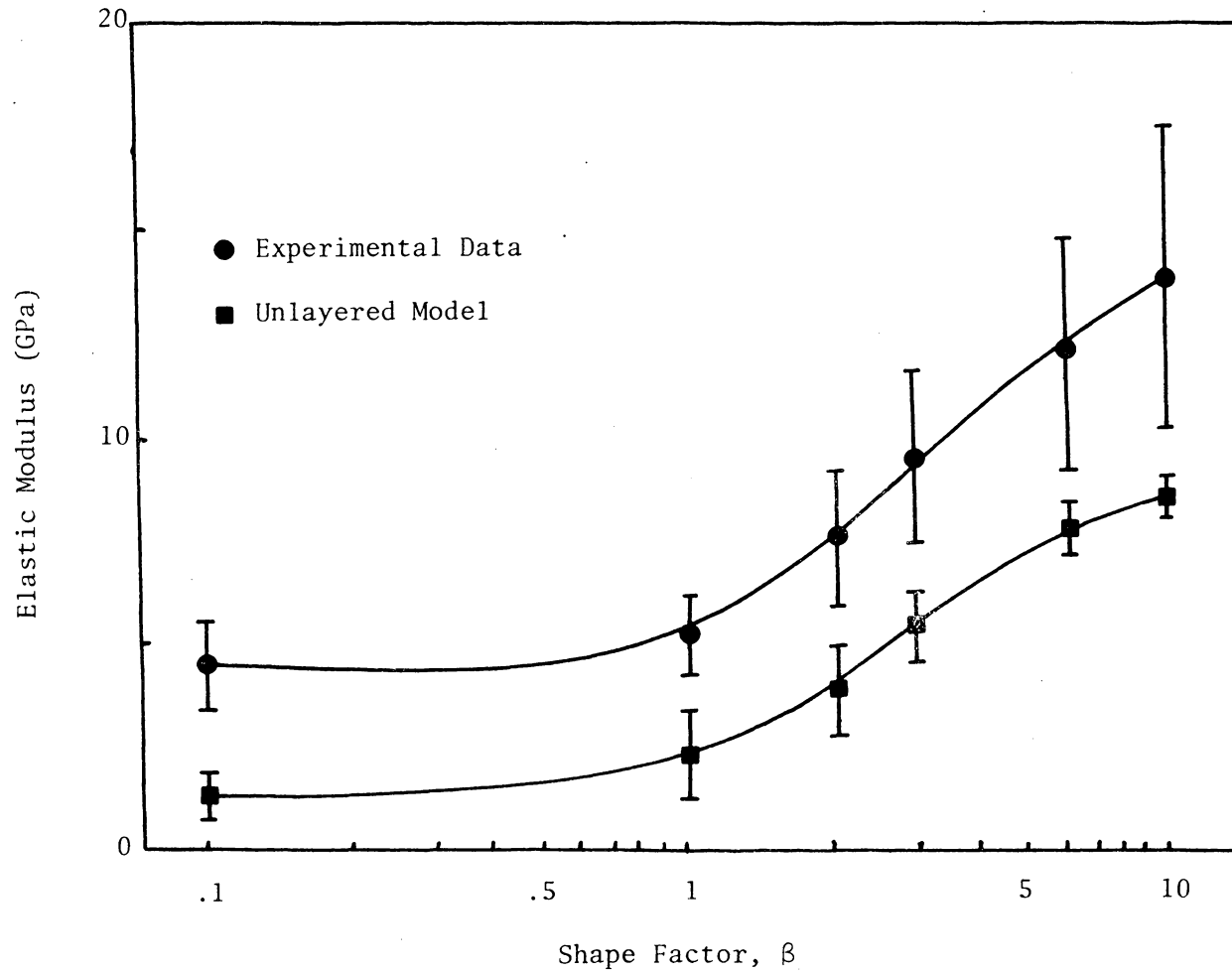


Figure 21. Tensile elastic modulus of white pine as a function of the degree of orientation.

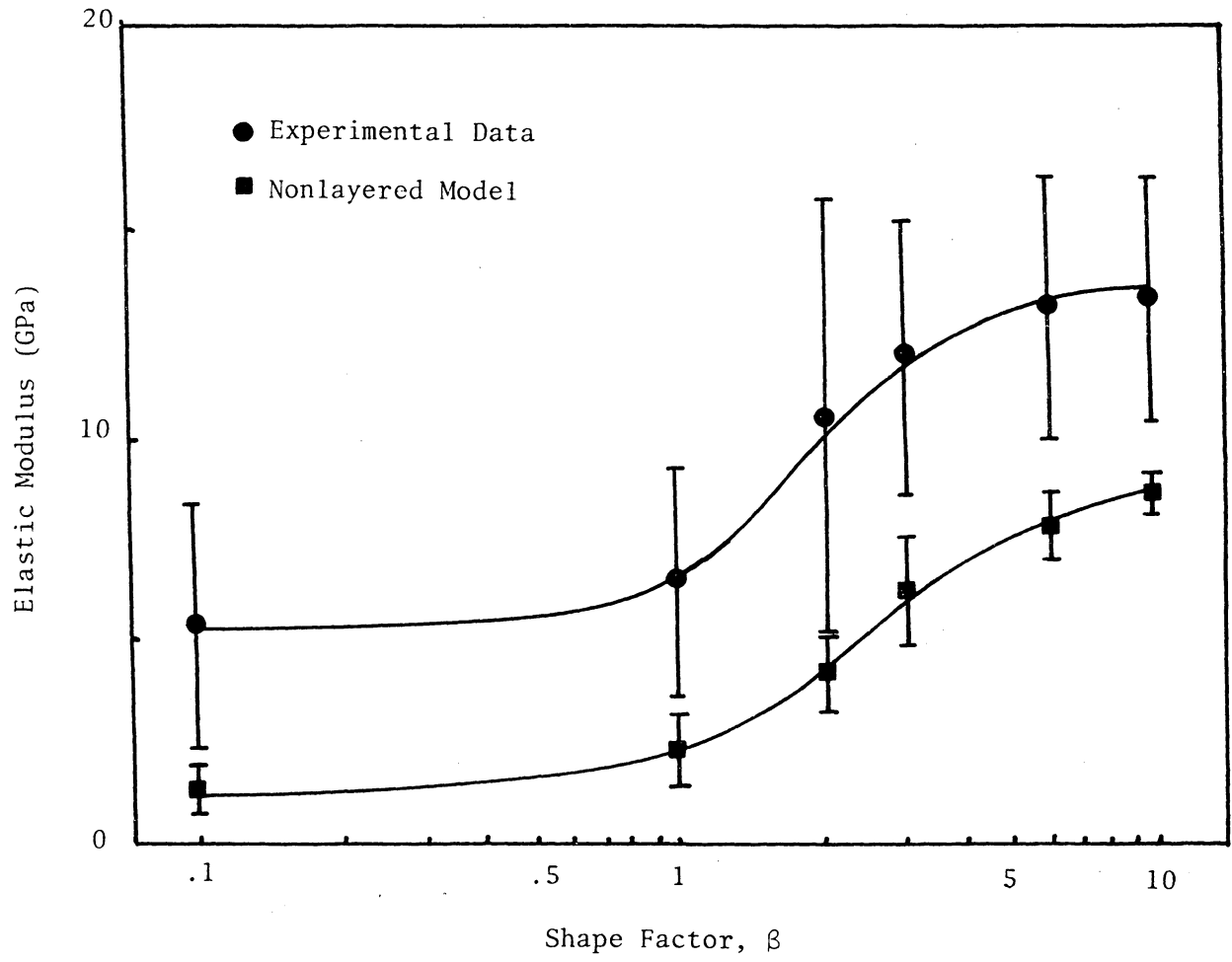


Figure 22. Tensile elastic modulus of aspen as a function of degree of orientation.

model should cause an increased elastic modulus at the lower levels of orientation.

The results of the densification and layering corrections are shown in Figures 23 and 24. The agreement between the measured and calculated specific moduli using the unlayered model is good for boards with greater degrees of orientation, however, at lower degrees of orientation the model predicts values noticeably lower than the experimental results. When calculations are made with the layered model, in this case the number of layers was assumed to be six, the predicted elastic constants at the lower degrees of orientation are raised, and are more representative of the measured values. A paired comparison analysis indicates good agreement between the calculated and measured values for both models when corrected for density, however, the layered model appears to be the more representative.

A comparison between the layered model and experimental E for the WSU boards is shown in Figure 25. As in the previous boards, the experimental and theoretical results are consistent, with a paired comparison showing no difference between the two (5 percent confidence level).

The Potlatch boards also showed a reasonable relationship between the specific E from the layered model, 15100 MPa and the experimental specific E, 17100 MPa.

It appears then, that the layered model can be used to estimate, with some success, the tensile elastic modulus of not only laboratory boards of known distribution, but also of commercial type boards with

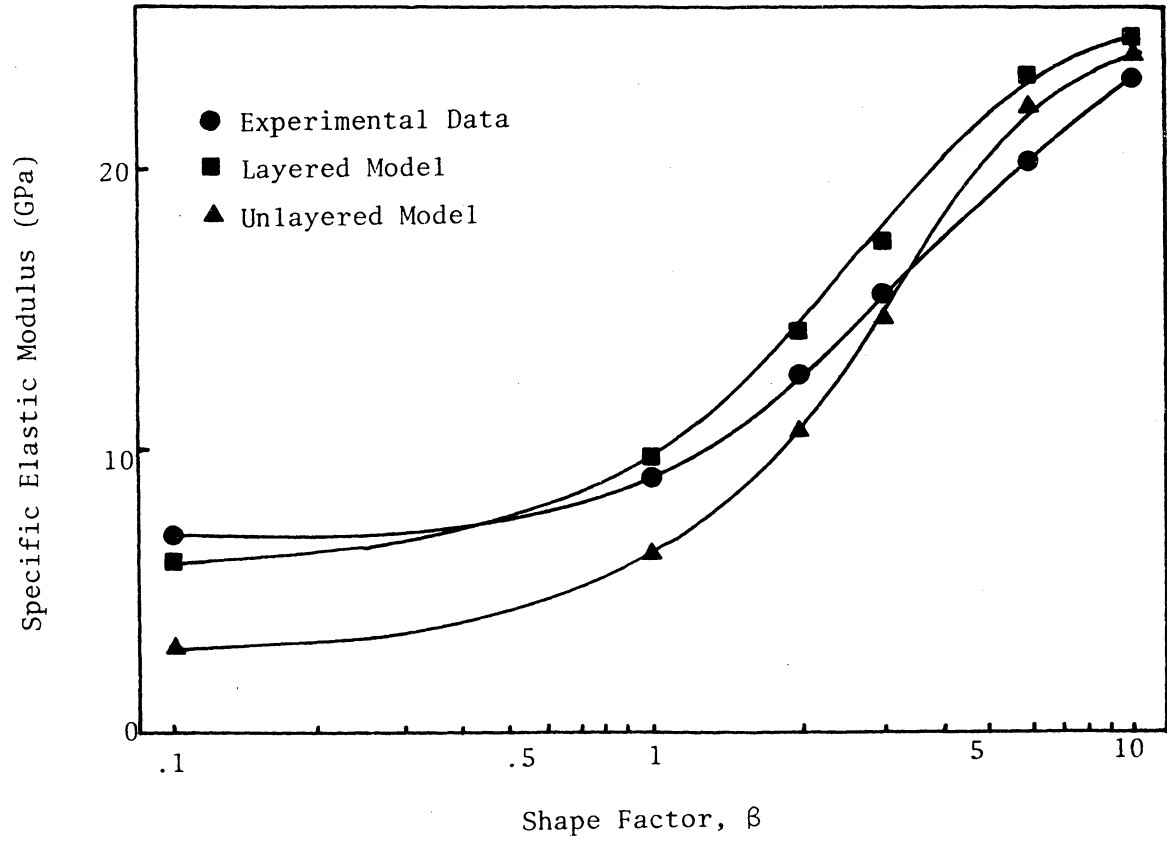


Figure 23. Specific tensile elastic modulus of white pine as a function of degree of orientation.

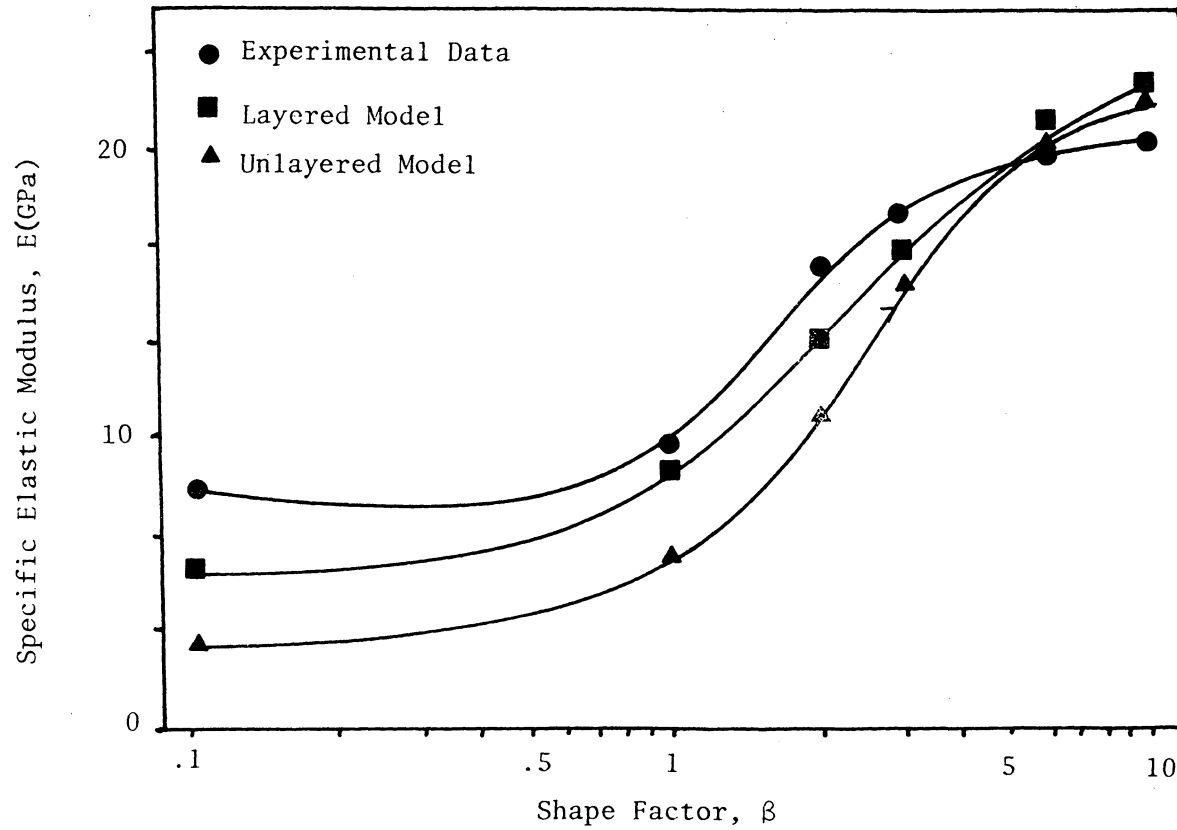


Figure 24. Specific tensile elastic modulus of aspen as a function of degree of orientation.

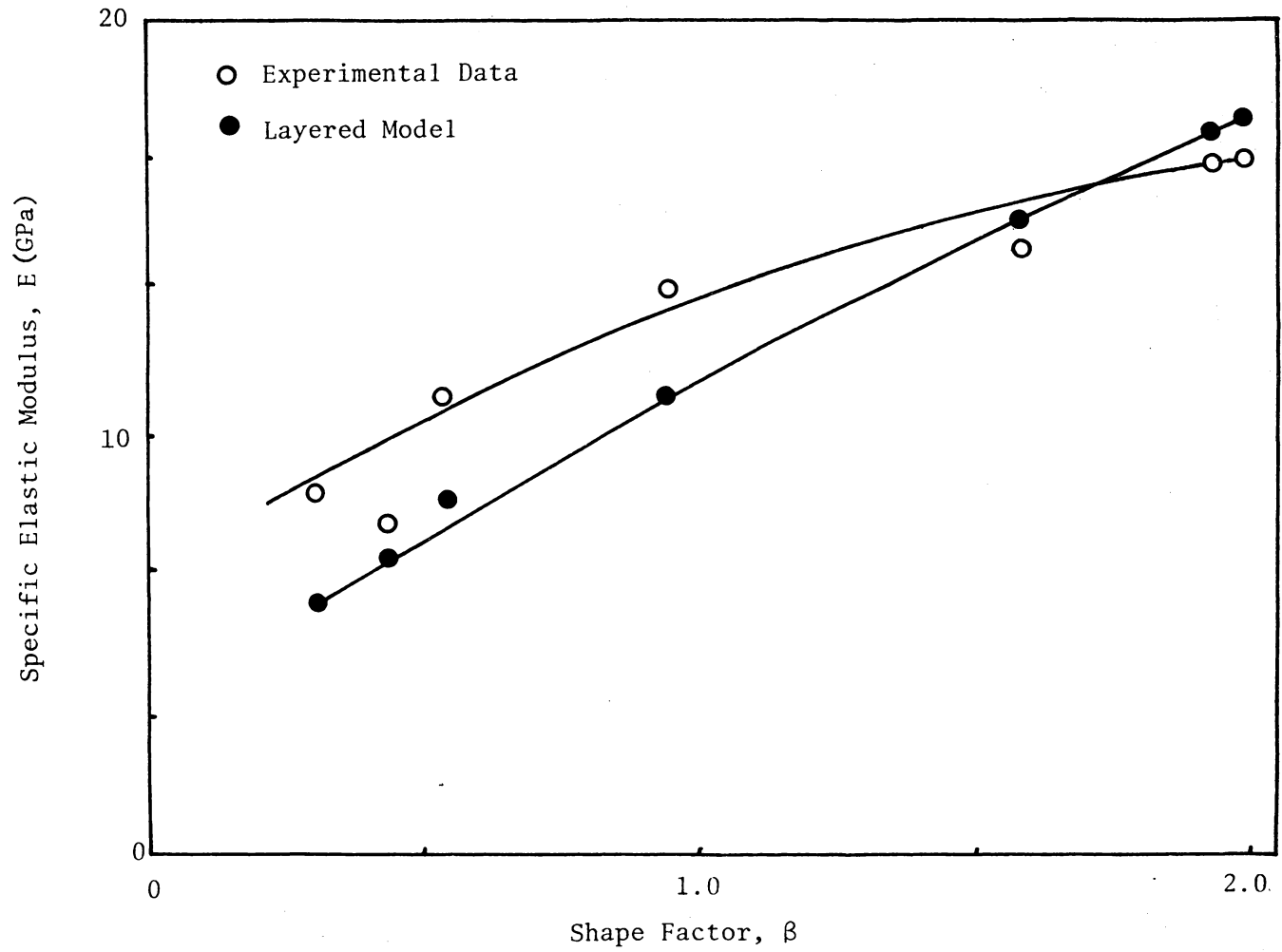


Figure 25. Specific tensile elastic modulus of WSU boards as a function of the degree of orientation.

unknown distributions when used in conjunction with the technique developed to estimate the orientation parameter.

Shear

For the boards with known distribution, the experimental shear results are in good agreement with the simulation results and are compared in Figures 26 and 27. The white pine data deviates more than the aspen, possible because the white pine boards were not pressed during cooling, and as a result, some of the boards were not perfectly flat. This was probably reflected in the results of the shear.

The theoretical and experimental results for the WSU boards are shown in Figure 28. Agreement between the two is poor, with a large discrepancy at both the high and low shape factors. This could be a result of the thickness of the WSU boards. The model is unlayered, and the idealized white pine and aspen boards were very thin (.08 inches), and agreement between experiment and theory was very good. The WSU boards, however, are .375 inches thick, and this could have caused the marked discrepancy.

The specific shear modulus for the theoretical and experimental tests were 1669 and 2069 ksi, respectively, for the Potlatch boards. Again, the lack of agreement could be the result of the board thickness and the over-simplification of the non-layered shear model.

Thus, it appears that the shear model works well for a thin idealized plate, however, for boards which are more representative of commercial products, the shear model does not predict satisfactory results.

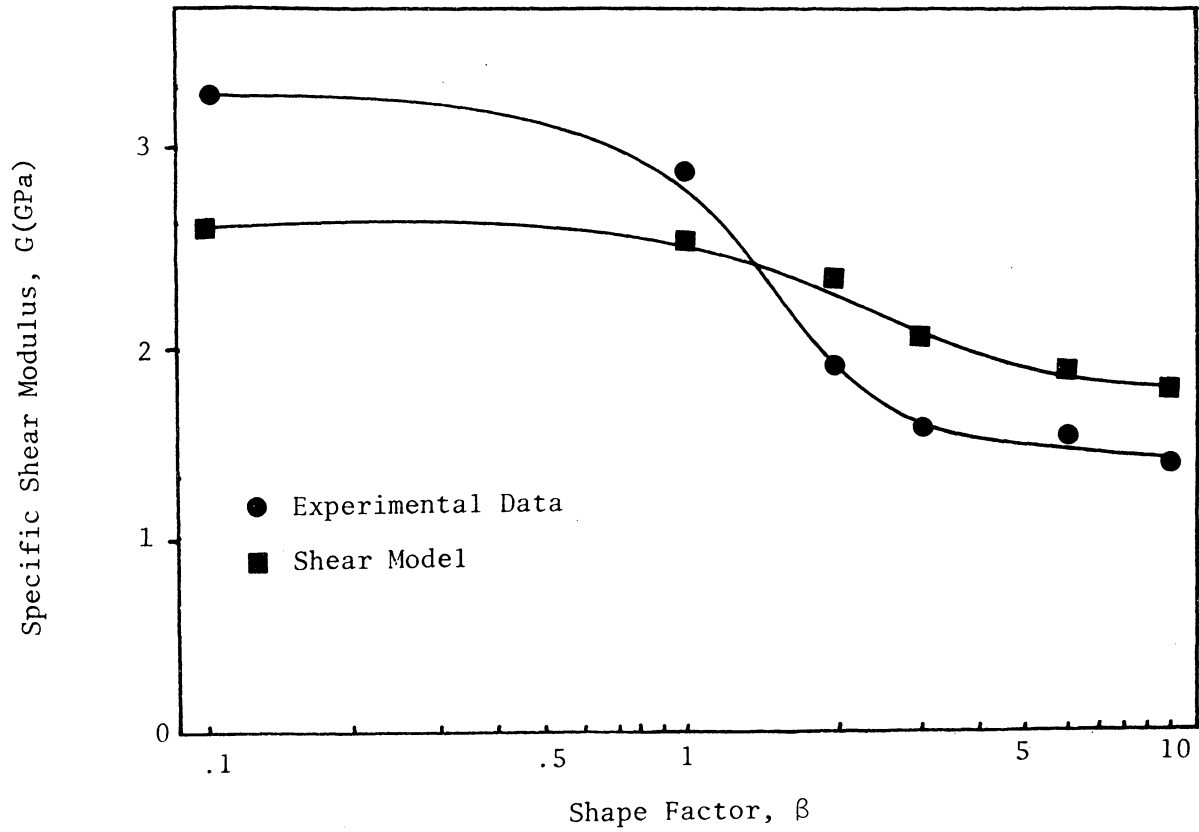


Figure 26. Specific shear modulus for white pine as a function of the degree of orientation.

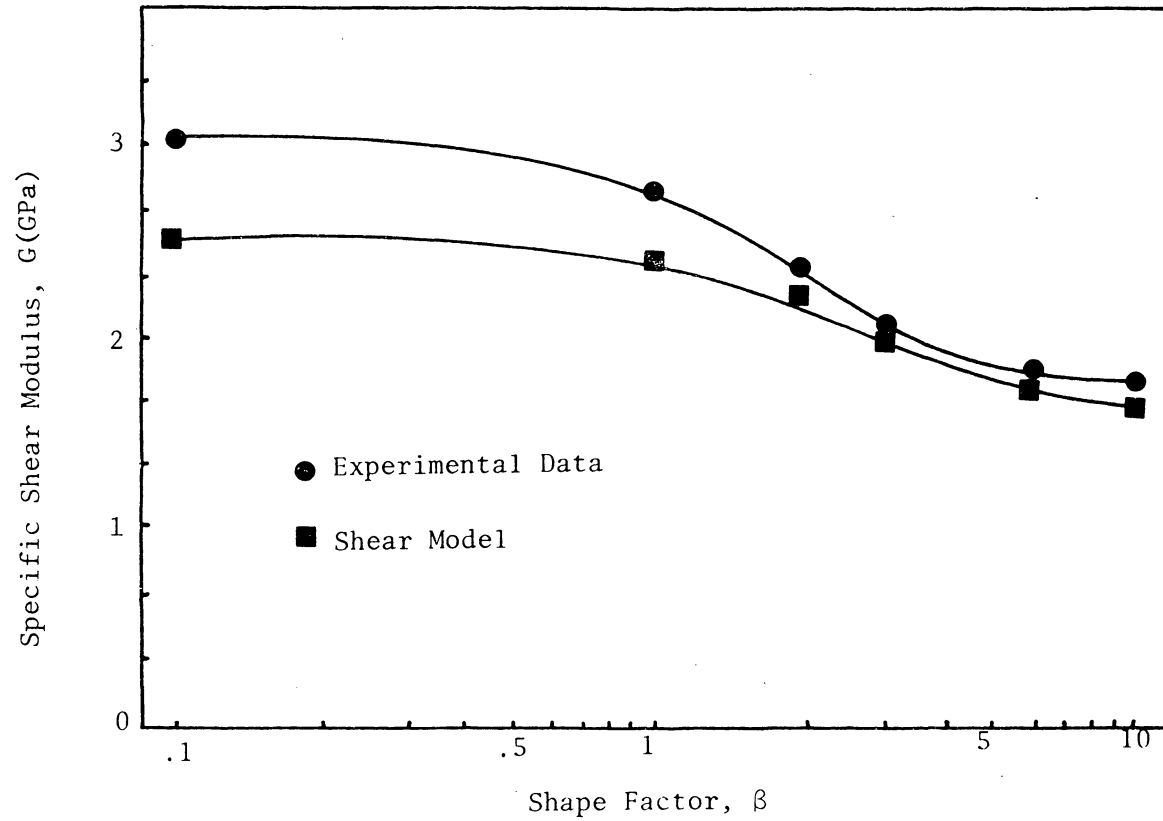


Figure 27. Specific shear modulus for aspen as a function of degree of orientation.

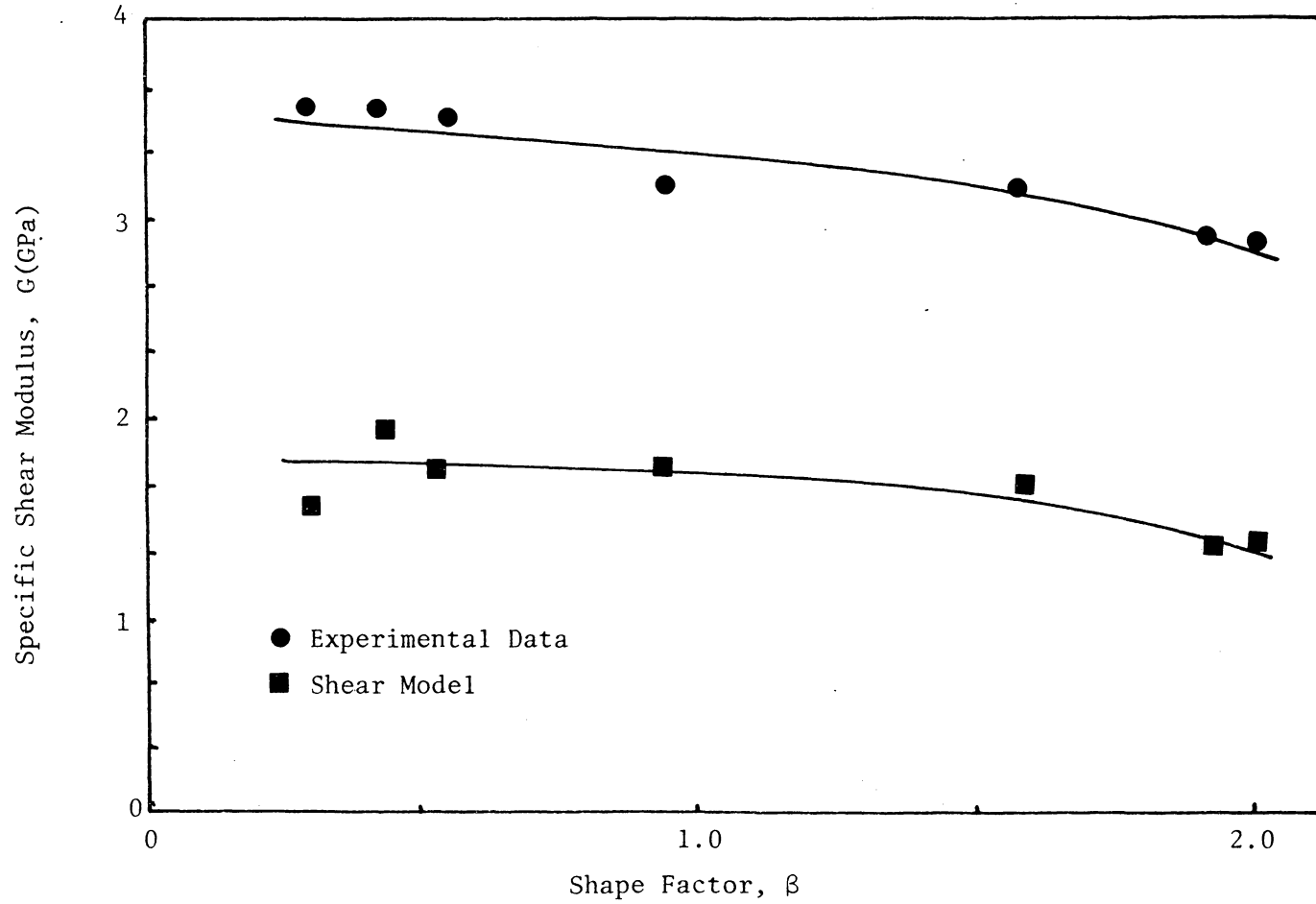


Figure 28. Specific shear modulus for WSU boards as a function of degree of orientation.

SUMMARY AND CONCLUSIONS

A method has been developed to determine the distribution of particle orientation in particleboard. This distribution can be expressed in terms of one parameter, the concentration parameter, k . The value of this approach lies in the quantitative measure of the degree of orientation, rather than a definition based on qualitative terms.

Models were developed and experimentally verified to predict the orientation effects on particleboard tensile stiffness. As expected, the tensile stiffness of the particleboard models increased as the orientation increased. The tensile elastic modulus of both layered and unlayered models more than tripled from a uniformly random distribution of particle angles to one in which the particles were nearly perfectly aligned.

The match between the tensile modulus of actual data and theoretical models was poor, however, when corrected for specific gravity, the actual and theoretical results were in close agreement. The layered model was in particularly good agreement with the experimental results, differing from the unlayered model by a marked increase in the tensile modulus at low degrees of orientation.

The tensile models worked well for all three types of boards used in the study: laboratory boards, pilot-scale boards (WSU) and commercial boards (Potlatch).

A shear model was used to predict the shear modulus of particleboard for various levels of particle orientation. The shear stiffness decreased up to 50 percent as the orientation increased from uniform

to highly oriented. Experimental data showed similar results. The shear model worked well for thin plates (.08 inches), however, the results for thick plates (.25 inches and greater) were not satisfactory, possibly due to the effects of layering which were not included in the model.

Other mechanical properties were experimentally determined and showed an increase with increasing orientation. They were: Poisson's ratio, MOE and MOR. The effects of particle length were also studied, and no effects were found which could be attributed to the length of the particles.

The results of this research represent a beginning to the understanding of the relationship between orientation and stiffness of particleboard from an analytical point of view. As results of this study indicate, the potential benefits of the orientation effects are not being approached by conventional orienting methods. It is hoped that more effort will be devoted to this type of research in the future to enable the wood scientist to design particleboards for specific end-use requirements.

REFERENCES

- American Society for Testing and Materials. 1974. ASTM Standards, Part 22 - Wood: Adhesives. Philadelphia, PA.
- Batschelet. 1965. Statistical methods for the analysis of problems in animal orientation and certain biological rhythms. American Institute of Biological Sciences, Washington, D.C. pp. 57.
- Beran, M. J. 1968. Statistical continuum theories. John Wiley and Sons, New York. pp. 424.
- Brumbaugh, J. 1960. Directional properties possible in flakeboards. The Lumberman. 87(7):46-47.
- Jayne, B. A. 1972. Theory and design of wood and fiber composite materials. Syracuse University Press, Syracuse, NY. 418p.
- Johnson, Jay A. 1973. Hygro-thermoplastic stresses in the transverse section of wood treated as a cylindrically orthotropic material. Ph.D. Diss., Univ. of Wash., Seattle, Washington.
- Johnson, Jay A. and Robert A. Harris. 1976. Characterizing particle orientation in particleboard with directional probability distribution functions and predicting the tensile elastic modulus. Report No. VPIWST-76-6, Virginia Polytechnic Institute and State University, Blacksburg, VA.
- Klanditz, W. 1960. Manufacture and properties of wood chip materials with directed strength. Holz als Roh und Werkstoff. 18(10): 377-385.
- Mardia, K. V. 1972. Statistics of directional data. Academic Press, New York. pp. 357.
- Steinmetz, P. E. and C. W. Polley. 1974. Influence of fiber alignment on stiffness and dimensional stability of high density dry-formed hardboard. Forest Prod. J. 24(5):45-50.
- Talbot, John W. 1976. Preparation of electrically oriented flakeboards of five discrete levels of orientation. WSU Research Report No. 76/57-23. Washington State Univ., Pullman, Washington.

APPENDIX A. Raw Data

The data collected from the experiment of this study is reproduced in the tables of this appendix.

Table A-1. Experimental tensile elastic modulus of white pine.

Tensile Elastic Modulus, E (MPa) ¹						
Sample Number	Shape Factor, β					
	0.1	1.0 ²	2.0 ²	3.0 ²	6.0 ³	10.0
1	5888 (854)	4302 (624)	6702 (972)	7536 (1093)	15520 (2251)	14348 (2801)
2	6336 (919)	5219 (757)	9722 (1410)	8715 (1264)	12369 (1794)	16334 (2369)
3	4192 (608)	5771 (837)	6881 (998)	10115 (1467)	9453 (1371)	14196 (2059)
4	3847 (558)	5674 (823)	7950 (1153)	12631 (1832)	10321 (1497)	12576 (1824)
5	3682 (534)	5936 (861)	8267 (1199)	6281 (911)		8942 (1297)
6	3351 (486)	3584 (520)	5295 (768)	10549 (1530)		8467 (1228)
7	3813 (553)	5371 (779)		9618 (1395)		16229 (2364)
8	3744 (543)					18926 (2745)
Mean	4357 (632)	5123 (743)	7467 (1083)	9349 (1356)	11914 (1728)	13762 (1996)
Standard Deviation	1117 (162)	869 (126)	1524 (221)	2082 (302)	2696 (391)	3647 (529)
Number of Samples	8	7	6	7	4	8

¹ Elastic Modulus, E, shown in ksi in parenthesis.

² Due to equipment malfunction, data from some of the eight samples was discarded. In one instance, a large void was present in a strip, and that strip was discarded.

³ Only four test strips were manufactured.

Table A-2. Experimental tensile elastic modulus of aspen.

Tensile Elastic Modulus, E (MPa) ¹						
Sample Number	Shape Factor, β					
	0.1	1.0	2.0	3.0	6.0	10.0
1	3902 (566)	3813 (533)	8136 (1180)	18000 (2611)	13424 (1947)	9253 (1342)
2	5171 (750)	10611 (1539)	6060 (879)	10432 (1513)	12976 (1882)	12521 (1816)
3	5805 (842)	3627 (526)	18085 (2623)	8908 (1292)	15148 (2197)	12066 (1750)
4	1813 (263)	4447 (645)	11307 (1640)	10184 (1477)	9529 (1382)	16782 (2434)
5	4537 (658)	6316 (916)	7053 (1023)	9797 (1421)	17506 (2539)	13790 (2000)
6	5378 (780)	7763 (1126)	9873 (1432)	7708 (1118)	6805 (987)	17237 (2500)
7	5206 (755)	9928 (1440)	6012 (872)	12521 (1816)	13969 (2026)	11342 (1645)
8	5206 (755)	4509 (654)	5026 (729)	14969 (2171)	15058 (2184)	11790 (1710)
9	13528 (1962)	5412 (785)	14093 (2044)	12879 (1868)	14700 (2132)	15692 (2276)
10			19395 (2813)		11611 (1684)	9520 (1382)
Mean	5612 (814)	6267 (909)	10508 (1524)	11714 (1699)	13072 (1896)	13004 (1886)
Standard Deviation	3199 (464)	2613 (379)	5143 (746)	3234 (469)	3082 (447)	2820 (409)
Number Of Samples	9	9	10	9	10	10

¹ Elastic Modulus, E, shown in ksi parenthesis.

Table A-3. Experimental Elastic modulus of WSU boards.

Tensile Elastic Modulus, E(MPa) ¹							
Board	Sample Number						
	1	2	3	4	5	6	7
A	5761 <i>836</i>	7569 <i>1098</i>	10357 <i>1502</i>	8764 <i>1271</i>	11920 <i>1729</i>	7477 <i>1084</i>	11399 <i>1653</i>
B	4934 <i>715</i>	7569 <i>1098</i>	9377 <i>1360</i>	10235 <i>1484</i>	10786 <i>1564</i>	6067 <i>880</i>	11828 <i>1716</i>
C	5350 <i>776</i>	7967 <i>1156</i>	7967 <i>1156</i>	9683 <i>1404</i>	11399 <i>1653</i>	5669 <i>822</i>	12104 <i>1756</i>
D	5792 <i>840</i>	7814 <i>1133</i>	8396 <i>1218</i>	9990 <i>1449</i>	11767 <i>1707</i>	5516 <i>800</i>	11828 <i>1716</i>
E	4992 <i>724</i>	7814 <i>1133</i>	9928 <i>1440</i>	10235 <i>1484</i>	11767 <i>1707</i>	5455 <i>791</i>	10296 <i>1493</i>
F	5853 <i>849</i>	7171 <i>1040</i>	10357 <i>1502</i>	11522 <i>1671</i>	11706 <i>1698</i>	6006 <i>871</i>	11798 <i>1711</i>
Mean	5474 <i>794</i>	7661 <i>1111</i>	9397 <i>1363</i>	10071 <i>1461</i>	11558 <i>1676</i>	6032 <i>875</i>	11542 <i>1674</i>
Standard Deviation	653 <i>95</i>	734 <i>106</i>	1495 <i>217</i>	1387 <i>201</i>	800 <i>116</i>	878 <i>127</i>	1459 <i>212</i>
Number of Samples	17	15	18	18	18	18	18

¹E in ksi shown in *italics*

Table A-4. Experimental shear modulus of WSU boards.

Plate Shear Modulus, G(MPa) ¹							
Board	Sample						
	1	2	3	4	5	6	7
A	2258 <i>371</i>	2471 <i>357</i>	2118 <i>307</i>	2213 <i>321</i>	2020 <i>293</i>	2507 <i>364</i>	2613 <i>379</i>
B	2365 <i>343</i>	2365 <i>343</i>	2165 <i>314</i>	2199 <i>319</i>	2068 <i>300</i>	2365 <i>343</i>	2165 <i>314</i>
C	2461 <i>357</i>	2461 <i>357</i>	2268 <i>329</i>	2117 <i>307</i>	2041 <i>296</i>	2558 <i>371</i>	2117 <i>307</i>
D	2558 <i>371</i>	2461 <i>357</i>	2117 <i>307</i>	2165 <i>314</i>	2117 <i>307</i>	2413 <i>350</i>	2020 <i>293</i>
E	2461 <i>357</i>	2489 <i>361</i>	2317 <i>336</i>	2186 <i>317</i>	2117 <i>307</i>	2413 <i>350</i>	2068 <i>300</i>
F	2461 <i>357</i>	2461 <i>357</i>	2213 <i>321</i>	2213 <i>321</i>	1937 <i>281</i>	2068 <i>300</i>	1937 <i>281</i>
Mean	2482 <i>360</i>	2448 <i>355</i>	2199 <i>319</i>	2186 <i>317</i>	2048 <i>297</i>	2482 <i>360</i>	2062 <i>299</i>
Standard Deviation	74 <i>11</i>	44 <i>6</i>	80 <i>12</i>	37 <i>5</i>	67 <i>10</i>	97 <i>14</i>	78 <i>11</i>
Number of Samples	6	6	6	6	6	6	6

¹MOE in ksi shown in *italics*

Table A-5. Modulus of elasticity of WSU boards.

Modulus of Elasticity in Flatwise Bending, MOE(MPa) ¹							
Board	Sample Number						
	1	2	3	4	5	6	7
A	5634 <i>817</i>	6584 <i>955</i>	8321 <i>1207</i>	9096 <i>1319</i>	11757 <i>1705</i>	4548 <i>660</i>	10643 <i>1544</i>
B	5390 <i>782</i>	6584 <i>955</i>	7738 <i>1122</i>	8254 <i>1197</i>	11512 <i>1670</i>	5838 <i>847</i>	9883 <i>1433</i>
C	4779 <i>693</i>	7304 <i>1059</i>	8566 <i>1242</i>	8485 <i>1231</i>	10535 <i>1528</i>	6652 <i>965</i>	10399 <i>1508</i>
D	5525 <i>801</i>	6177 <i>896</i>	9001 <i>1305</i>	10290 <i>1492</i>	9530 <i>1382</i>	5836 <i>847</i>	9924 <i>1439</i>
E	4371 <i>634</i>	6489 <i>941</i>	9910 <i>1437</i>	9001 <i>1305</i>	10439 <i>1514</i>	5905 <i>857</i>	9775 <i>1418</i>
F	4575 <i>664</i>	6109 <i>886</i>	8227 <i>1193</i>	9041 <i>1311</i>	10182 <i>1477</i>	5345 <i>776</i>	11173 <i>1620</i>
Mean	5046 <i>731</i>	6541 <i>949</i>	8627 <i>1252</i>	9028 <i>1309</i>	10659 <i>1546</i>	5688 <i>825</i>	10299 <i>1493</i>
Standard Deviation	728 <i>106</i>	479 <i>69</i>	1043 <i>151</i>	745 <i>108</i>	869 <i>126</i>	760 <i>110</i>	722 <i>105</i>
Number of Samples	12	12	12	12	12	12	12

¹MOE in ksi shown in *italics*

Table A-6. Modulus of rupture of WSU boards.

Modulus of Rupture in Flatwise Bending, MOR(MPa) ¹							
Board	Sample						
	1	2	3	4	5	6	7
A	43.3 <i>6291</i>	45.3 <i>6570</i>	58.5 <i>8485</i>	58.0 <i>8421</i>	71.0 <i>10421</i>	30.0 <i>4344</i>	68.5 <i>9940</i>
B	34.8 <i>5050</i>	40.4 <i>5853</i>	51.6 <i>7490</i>	40.7 <i>5906</i>	76.0 <i>11117</i>	40.4 <i>5863</i>	55.9 <i>8110</i>
C	31.2 <i>4526</i>	53.0 <i>7682</i>	56.4 <i>8175</i>	50.9 <i>7394</i>	58.2 <i>8442</i>	43.5 <i>6302</i>	68.7 <i>9961</i>
D	36.6 <i>5318</i>	43.5 <i>6302</i>	59.2 <i>8592</i>	68.3 <i>9919</i>	56.9 <i>8250</i>	38.0 <i>5510</i>	61.3 <i>8892</i>
E	29.0 <i>4216</i>	46.0 <i>6677</i>	67.4 <i>9769</i>	57.8 <i>8389</i>	63.9 <i>9277</i>	42.1 <i>6110</i>	55.5 <i>8057</i>
F	28.0 <i>4055</i>	39.8 <i>5777</i>	50.8 <i>7361</i>	48.9 <i>7094</i>	62.7 <i>9095</i>	33.3 <i>4836</i>	68.9 <i>9994</i>
Mean	33.8 <i>4909</i>	44.7 <i>6477</i>	57.3 <i>8312</i>	54.1 <i>7854</i>	65.0 <i>9434</i>	37.9 <i>5494</i>	63.1 <i>9159</i>
Standard Deviation	7.1 <i>1024</i>	5.5 <i>803</i>	9.0 <i>1308</i>	9.8 <i>1416</i>	9.7 <i>1405</i>	6.2 <i>892</i>	8.6 <i>1246</i>
Number of Samples	12	12	12	12	12	12	12

¹MOR in psi shown in *italics*

APPENDIX B. Statistics Results

Table B-1. ANOVA results showing no significant difference between selected mechanical properties of boards having two different aspect ratios.

	Source	df	Mean Square	F
Tension	Random .75 vs 1.5	1	26526230203	.9144
	Oriented .75 vs 1.5	1	444444444	.0015
	Error	35	29009998216	
Shear	Random .75 vs 1.5	1	0	0
	Oriented .75 vs 1.5	1	10884720	.1024
	Error	35	106271795	
MOE	Random .75 vs 1.5	1	52116437626	2.8729
	Oriented .75 vs 1.5	1	16335494689	.9005
	Error	35	18140506528	
MOR	Random .75 vs 1.5	1	2052793	1.0972
	Oriented .75 vs 1.5	1	452521	.2419
	Error	35	1870972	

**The vita has been removed from
the scanned document**

MEASURING PARTICLE ALIGNMENT IN PARTICLEBOARD AND
PREDICTING SELECTED MECHANICAL PROPERTIES
OF ORIENTED BOARDS

by

Robert A. Harris

(ABSTRACT)

Particle orientation in particleboard was characterized by two directional distribution functions, the von Mises and truncated gaussian. This approach has the advantage of characterizing the degree of orientation by specifying only one parameter. A method was developed to measure the orientation of particles in particleboard "in situ", and to express the orientation in terms of the direction distribution functions.

Models were developed to compute the tensile and shear modulus of particleboard with various degrees of orientation. The tensile model worked well for several board types. The shear model, however, was only effective for thin plates. Poisson's ratio, the tensile modulus, modulus of elasticity, and modulus of rupture increased in the direction of particle alignment as the degree of orientation increased. The shear modulus decreased as the orientation increased.

The results indicate that conventional methods of orienting particles must be greatly refined before the potential benefits of orientation are realized.